*Acta Geologica Polonica*, Vol. 69 (2019), No. 4, pp. 489–511
DOI: 10.24425/agp.2019.126445

# U-Pb zircon geochronology of high-grade charnockites – exploration of pre-Mesoproterozoic crust in the Mazury Complex area

EWA KRZEMIŃSKA[1], ALEKSANDRA ŁUKAWSKA[1] and BOGUSŁAW BAGIŃSKI[2]

[1] *Polish Geological Institute-National Research Institute, Rakowiecka 4, PL-00-975 Warszawa, Poland.*
*E-mails: ewa.krzeminska@pgi.gov.pl; aleksandara.lukawska@pgi.gov.pl*
[2] *Faculty of Geology, University of Warsaw, Żwirki i Wigury 93, PL-02-089 Warszawa, Poland.*
*E-mail: baginski1@uw.edu.pl*

ABSTRACT:

Krzemińska, E., Łukawska, A. and Bagiński, B. 2019. U-Pb zircon geochronology of high-grade charnockites – exploration of pre-Mesoproterozoic crust in the Mazury Complex area. *Acta Geologica Polonica*, **69** (4), 489–511. Warszawa.

Charnockites – i.e., orthopyroxene-bearing felsic rocks – were formed in a deep-seated dry environment, either under plutonic or high-grade metamorphic conditions. Most charnockites known from the crystalline basement of Poland appear to be of Mesoproterozoic age (1.50–1.54 Ga), cogenetic with the Suwałki Anorthosite Massif, and associated with mangerite and granite members forming the AMCG suite of the Mazury Complex. Genetically distinct rocks, characterised by the presence of anhydrous minerals, e.g., orthopyroxene and garnet, were also recognised along 592 m of the Łanowicze PIG-1 borehole section, within the AMCG suite. U-Pb geochronology by sensitive high resolution ion microprobe (SHRIMP) was used to date the complexly zoned zircons. The ages of crystallisation of the charnockite protoliths from various depths at 1837±7, 1850±9, 1842±6, and 1881±16 Ma makes these rocks the oldest dated crust within this part of the Polish basement. The Łanowicze PIG-1 borehole section bears components from neighbouring tectonic domains known from Lithuania: the West and Middle Lithuanian (WL/MLD) domains considered as a continental margin at 1.84–1.86 Ga and the fragmented Latvia-East Lithuania (LEL) domain, where the oldest continental crust was generated at c. 1.89–1.87 Ga. The metamorphic zircon overgrowths document a high-grade event at 1.79 Ga and then constrained at 1.5 Ga. Dating of pre-Mesoproterozoic crust cryptic within the AMCG Mazury Complex provides valuable information on the nature of the pre-existing blocks formed during the long lasting Svecofennian orogeny.

**Key words:** Magmatic protolith; SHRIMP dating; Dry metamorphism; Svecofennian orogeny; Active continental margin.

## INTRODUCTION

Charnockites, with orthopyroxene-bearing mineral assemblages, are components of magmatic suites and many high-grade terrains. A magmatic *versus* metamorphic origin of charnockites is still a matter of debate (Frost and Frost 2008; Rajesh and Santosh 2012; Grantham *et al*. 2012 and references therein). It has been recognised that stabilisation of orthopyroxene relative to biotite in granitic rocks is a function of low $aH_2O$, high temperature and composition, especially the Fe/(Fe+Mg) whole-rock ratio. This requires that threshold conditions can be met by mantle-derived hot differentiated melts or varieties of subsolidus metamorphic, metasomatic processes. Charnockites also occur in high pressure and

high temperature metamorphic regimes, and thus may preserve the record of deep crustal processes (Janardhan *et al.* 1982; Frost *et al.* 2000).

In the Precambrian basement of NE Poland, charnockites were generated in the Mazury Complex (MC), which is a key area for orthopyroxene-bearing magmatic rocks in this part of the East European Craton (EEC), appearing together with other contemporaneous anorthosite-mangerite-charnockite-granite rocks that form an AMCG suite (Bagiński and Krzemińska 2004, 2005; Bogdanova *et al.* 2006; Skridlaite *et al.* 2008).

The AMCG assemblage was emplaced during the Mesoproterozoic along E–W-trending lineaments within the basement of NE Poland and adjacent southern Lithuania (Text-fig. 1). Several examples of such rocks were recovered from different depths of the Pawłówka PIG-1 and Bilwinowo IG-1 deep boreholes (Text-fig. 2), situated close to the Suwałki Anorthosite Massif (SAM), where the Krzemianka-Udryń ilmenite-magnetite ore deposits are hosted in anorthosites. The crystallisation age of the charnockite at 1540±30 Ma (Bilwinowo IG-1) obtained by the chemical method on monazites (Bagiński 2006) does not differ (within error range) from the major time of formation of the AMCG pluton between 1.53–1.50 Ga (Wiszniewska *et al.* 2016).

A subsequent monazite chemical age investigation in the Mazury area determined an age of ~1.82 Ga for an older charnockitic rock type. The rocks were derived from the Łanowicze PIG-1 borehole section (Bagiński 2006), which is located almost in the centre of the AMCG suite. This borehole was drilled about 6 km to the west of the Krzemianka-Udryń Fe-Ti-V ore deposit, where the Re-Os isochron method indicated a mineralisation age of 1559±37 and 1556±94 Ma (Morgan *et al.* 2000), and 4 km east of Filipów, where U-Pb zircon SIMS analyses yielded an emplacement age of the rapakivi granitoids at 1512±17 Ma (Wiszniewska *et al.* 2016). Within that spatial and geological context, we attempted a precise age dating of zircons from the charnockite-dominated Łanowicze PIG-1 borehole section. This dating should resolve the problem of the time of charnockite generation and the enigmatic nature of the unknown pre-AMCG basement in this area, completing regional correlations in the platform area of the EEC, where field relationships are obscured.

## REGIONAL CONTEXT

The crystalline basement of NE Poland and adjacent countries (Lithuania, Belarus, Latvia, Estonia) is characterised by an array of alternating belt-shaped tectonic domains (Bogdanova *et al.* 2015; Text-fig. 1), formed mostly in Palaeoproterozoic time and completed in the Mesoproterozoic (Bogdanova *et al.* 2006, 2015 and references therein; Krzemińska *et al.* 2017). Investigations of the crystalline rocks in this area were based on material from boreholes; they have revealed that the generation of mostly late Palaeoproterozoic juvenile crustal belts occurred successively, concomitantly with continuing accretion becoming progressively younger towards the southwest.

The Lithuanian crystalline basement is subdivided into the West Lithuanian granulite domain (WL), being a part of Amberland, the Middle Lithuanian domain as a part of the Mid-Baltic belt (MLD), and the Latvia-East Lithuania (LEL) belt genetically related with a much more extensive unit including Bergslagen in Sweden as well as part of southern Finland (Text-fig. 1). Most of the crystalline basement in East Lithuania, e.g., the LEL, was formed at c. 1.89 Ga in a volcanic arc environment (Bogdanova *et al.* 2015; Siliauskas *et al.* 2018b). These rocks were later metamorphosed under amphibolite facies conditions. The western part of the area, including the WL granulite domain, was formed later. The oldest generation of plutonic rocks, emplaced at c. 1.85–1.81 Ga, form the Kuršiai (Curonian) batholith and a few smaller bodies (Motuza *et al.* 2008). In contrast, in the adjacent Polish basement the domains are characterised by a voluminous younger, c. 1.83–1.80 Ga, plutonic and volcanic magmatism marked by a subduction-related geochemistry (Krzemińska *et al.*

Text-fig. 1. Sketch of the East European Craton (EEC), showing the distribution of major crustal domains within its western part; from → Bogdanova *et al.* (2015), modified by Krzemińska *et al.* (2017). Symbols: BB – Bothnian Basin, BS – Bergslagen area, BPG – Belarus-Podlasie granulite belt, CFAC – Central Finland Arc Complex, CFGC – Central Finland Granitoid Complex, DD – Dobrzyń domain, DM – Mazowsze domain, MC – Mazury complex, LA – Latgalia domain, LEL – Latvian-East Lithuanian domain, LKO – Lapland-Kola orogen, LS – Ljusdal domain, MLD – Mid-Lithuanian domain, NB – Norrbotten Craton, NO – Novgorod domain, OH – Okołowo-Holeszów belt, O-J – Oskarshamn-Jönköping belt, OMI – Osnitsk-Mikashevichi Igneous Belt, PB – Pomorze-Blekinge belt, RB – Riga batholith, SEG – South Estonian granulite domain, SFS – Fennoscandia-Sarmatia suture, TN – Tallinn domain, TTZ – Teisseyre-Tornquist Zone, VV – Västervik domain, WE – West Estonian domain, WL – West Lithuanian domain. Locations of the Łanowicze PIG-1 borehole and the Lithuanian Kuršiai batholith are shown. A proposed crustal structure in the southern part of the Svecofennian orogen integrated across the Baltic Sea with the scope of the hypothetical Amberland and Mid-Baltic belt as newly created microcontinents (*sensu* Bogdanova *et al.* 2015), are also marked

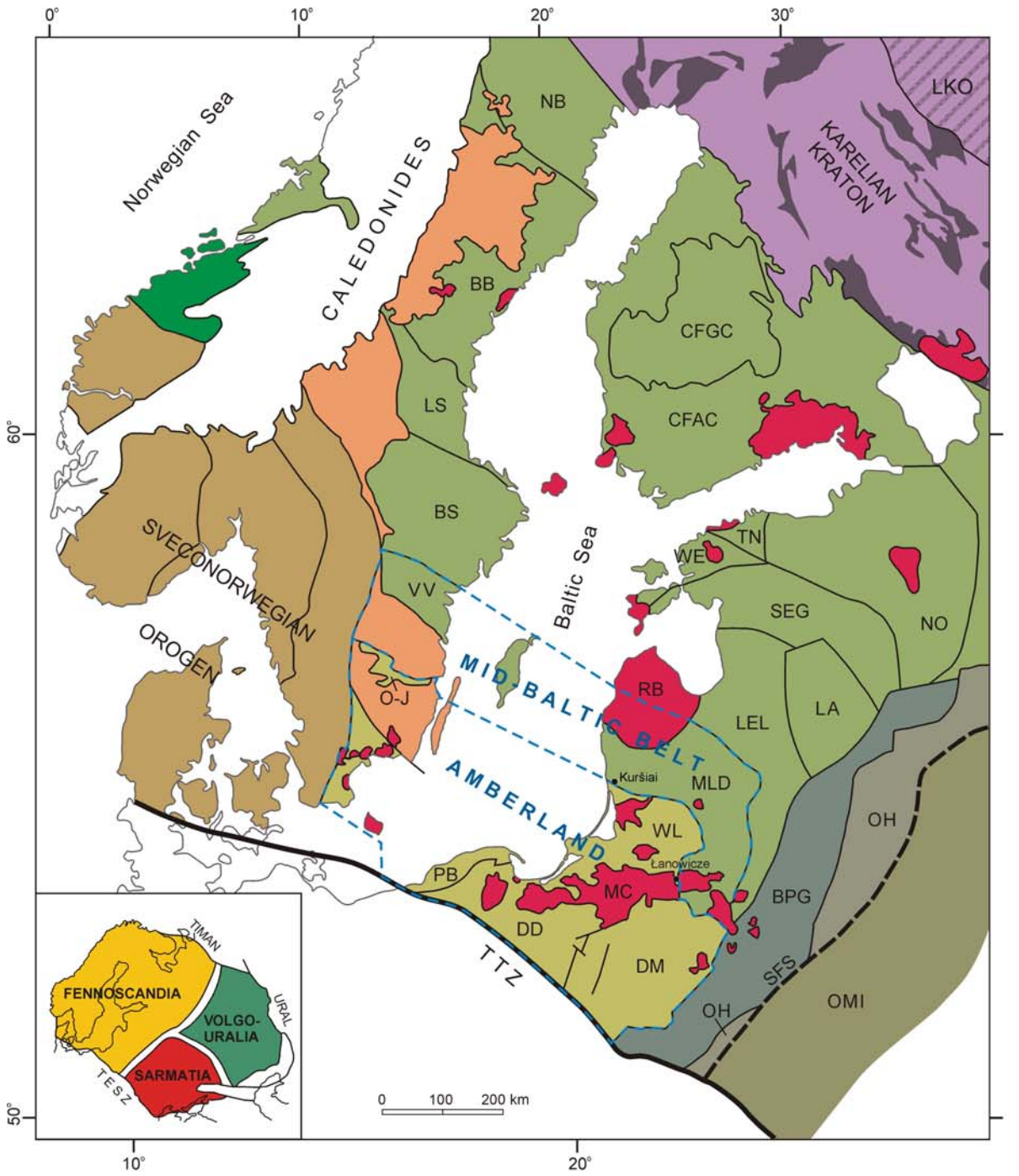
0°
10°
20°
30°
60°
50°
Norwegian Sea
CALEDONIDES
NB
LKO
KARELIAN KRATON
BB
CFGC
LS
CFAC
BS
TN
WE
SVECONORWEGIAN OROGEN
Baltic Sea
VV
SEG
NO
MID-BALTIC BELT
RB
O-J
LEL
LA
AMBERLAND
Kuršiai
MLD
OH
WL
Łanowicze
PB
MC
BPG
DD
TTZ
DM
SES
OH
OMI
0 100 200 km
TIMAN
FENNOSCANDIA
VOLGO-URALIA
URAL
SARMATIA
TESZ
Palaeo- to Mesoproterozoic crust reworked during the Sveconorwegian orogeny (1.14–0.92 Ga)
AMCG suites (1.65–1.44 Ga)
Transscandinavian Igneous Belt (1.81–1.75 Ga)
Palaeoproterozoic crust of Fennoscandia:
1.69–1.65 Ga
1.85–1.74 Ga
1.95–1.85 Ga
Palaeoproterozoic crust of Sarmatia:
1.9–1.85 Ga
2.0–1.9 Ga
2.0–1.95 Ga
Lapland-Kola collisional orogen (1.91–1.88 Ga)
Archaean to Palaeoproterozoic supracrustal rocks (2.6–1.96 Ga)
Archaean crust (3.5–2.6 Ga)

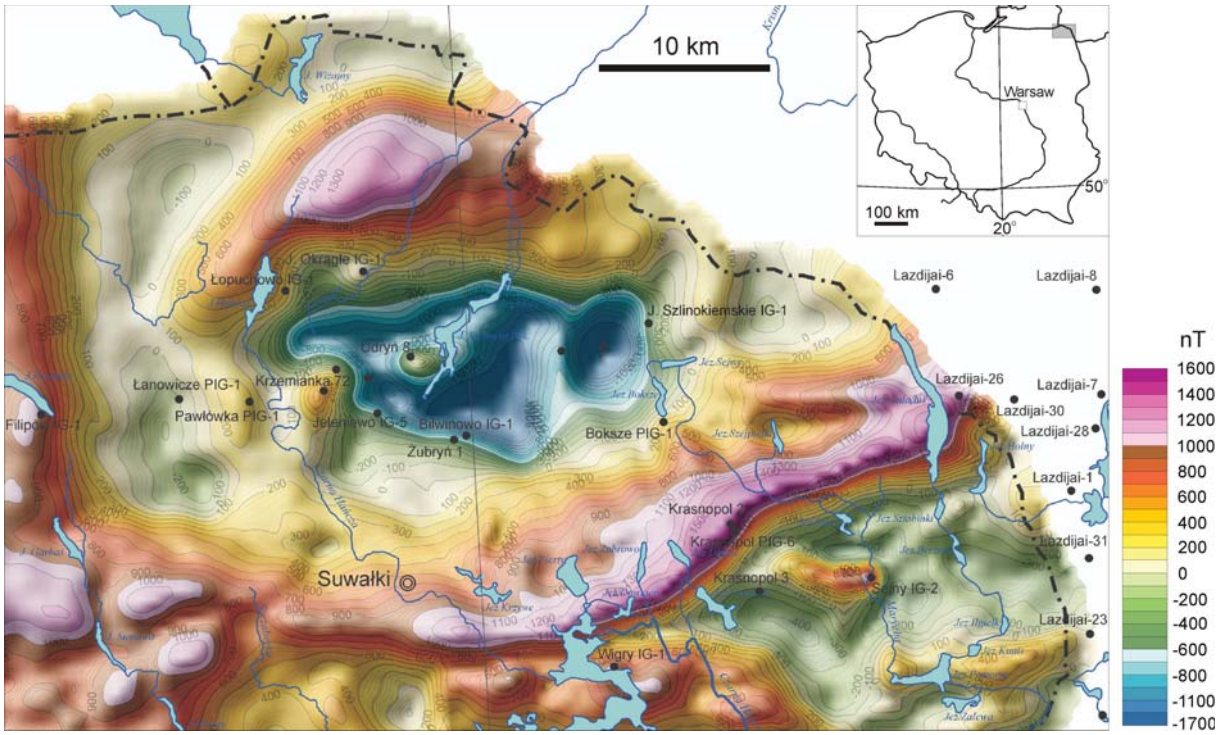


Text-fig. 2. Magnetic anomalies of the crystalline basement of the north-easternmost part of Poland plotted on a topographic map (Wybraniec 1999), showing the area of the Suwałki Anorthosite Massif with the location of the sampling site: Łanowicze PIG-1 and selected boreholes of the AMCG suite: Bilwinowo IG-1, Pawłówka PIG-1, Filipów IG-1, Boksze IG, and the group of Krzemianka, Jeleniewo and Lazdijai 8 (Lithuania) boreholes

2005, 2017). The WL reveals a composite crustal nature dominated by charnockitoids and rocks with felsic, and intermediate metavolcanic and sedimentary protoliths (Skridlaite and Motuza 2001; Motuza 2005) affected by high-grade metamorphic and retrogressive events at 1.80–1.79, 1.73–1.68, 1.62–1.58 and 1.52–1.50 Ga (see Skridlaite *et al.* 2014).

The WL is bordered by the 1.86–1.84 Ga MLD, known also as the Mid-Lithuanian Suture Zone (MLSZ). It represents a zone of rapid lateral changes of crustal structure, where the Moho gradually deepens from 40 to 50 km (Motuza *et al.* 2008) and volcano-plutonic mafic and felsic rocks displaying a subduction-related geochemical signature were recognised (Motuza 2005). In this convex belt, ranging in width from about 100 km in the NW to 20 km in the SE, the WL and MLD rocks occur together. In consequence, such a prominent zone, characterised by contrasting gravity and magnetic anomalies and low-velocity layers at depths of 120–150 km, has been interpreted in Lithuania as a palaeo-subduction zone (Janutyte *et al.* 2015). The available age determinations (Bogdanova *et al.* 2015) and chemistry of the igneous rocks in the MLD characterise this domain as an active continental margin at 1.86–1.84 Ga.

The southern boundaries of MLD and WL are blurred by a younger, Mesoproterozoic, E–W-trending chain of anorogenic intrusions of a AMCG suite that extends c. 200–300 km to the east from northern Poland (e.g., the Mazury Complex) to southern Lithuania (e.g., Kabeliai) and NW Belarus (Skridlaite *et al.* 2003). The AMCG suite was emplaced episodically, between 1.53 and 1.50 Ga (Dörr *et al.* 2002; Wiszniewska *et al.* 2007, 2016). This area of a deeply-buried basement was intensively penetrated by numerous boreholes (c. 104 deep drillings), but the majority document the area of the SAM, because of their potential as sources of Fe-Ti-bearing ferrolitic ores (Wiszniewska 2002). The anorthosite massif is associated with porphyritic (rapakivi texture) A-type and hornblende-bearing granitoids and coeval orthopyroxene-bearing granitoids (mangerites and charnockites).

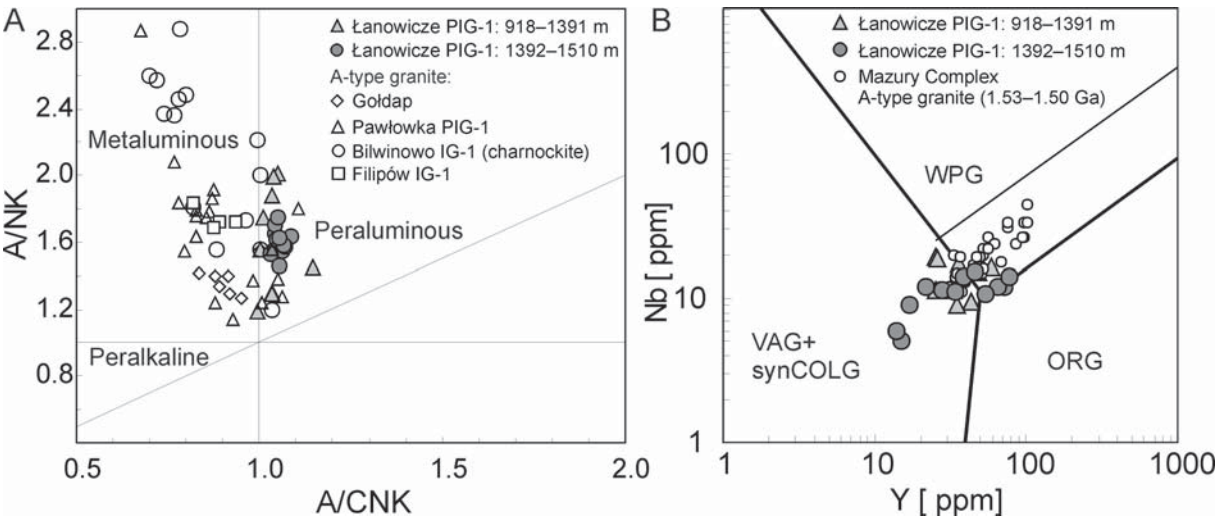


Text-fig. 3. Basic geochemical features of the Łanowicze PIG-1 borehole charnockites. A – diagram from Maniar and Piccoli (1989); B – discrimination diagram of granite tectonic setting (Pearce *et al*. 1984) with intrusive settings: described as ocean ridge granites (ORG), volcanic arc granites (VAG), within-plate granites (WPG) and collision granites (COLG). Data taken from Bagiński *et al*. (2001) and Suppl. Table 1 (all supplementary tables are available only in online version)

**Charnockitic rocks**

Of the possible mechanisms that form charnockites (Frost and Frost 2008; Grantham *et al.* 2012), the generation of anhydrous, opx-bearing rocks can be related either to dry magmatic crystallisation or to dry high-grade metamorphism (granulite facies). A number of genetic models and their variations have been discussed over the years, including:

– magmatic charnockites, generated from high temperature magmas with low $aH_2O$, with crystallisation of orthopyroxene (Stern and Dawoud 1991; Kilpatrick and Ellis 1992);
– metamorphic charnockites, being anhydrous restites of lower crust material from which partial melts have been removed (Clemens 1992);
– metamorphic charnockites formed during granulite facies metamorphism under fluid-present conditions of low oxygen fugacity and high partial pressures of carbon dioxide, involving the breakdown of hydrous mafic phases and the generation of orthopyroxene (Hansen *et al.* 1987, 1995);
– metasomatic charnockites formed by the dehydration of hydrous minerals by brines (Perchuk and Gerya 1993; Aranovich and Newton 1995);
– metamorphic charnockites formed by thermal desiccation in aureoles adjacent to hot anhydrous intrusions emplaced into granitic rocks (Van der Kerkhof and Grantham 1999).

Hence, the main occurrences of these opx-bearing rocks can be related mainly to:

– igneous AMCG suites all around the world (Duchesne and Wilmart 1997; Frost *et al.* 2000), where they represent the most dry components of silicic members;
– high-grade metamorphic terranes, mainly Proterozoic, under conditions close to the granulite facies limit;
– rocks that could be the result of charnockitisation caused by $CO_2$-rich fluids (Kleinefeld and Olesch 2000); and
– products of C-type magmas (Kilpatrick and Ellis 1992).

Undoubtedly, the most important factor remains the stability of orthopyroxene relative to biotite in granitoid-type rocks. It is a function of low $aH_2O$ (± high $CO_2$), composition, especially Fe/(Fe+Mg), and high temperature (Gratham *et al.* 2012 and references therein).

At least two genetic types of charnockitic rocks have been recognised within the Precambrian basement of NE Poland (Bagiński and Krzemińska 2004). Those occurring within the SAM, mostly found in the Bilwinowo IG-1 borehole (Text-fig. 2), are magmatic, connected with a suite of anorogenic intrusions generally emplaced between c. 1.53 and 1.50 Ga and composed of anorthosite and hornblende-bearing granitoid bodies, characterised by metaluminous, ferroan and

high $K_2O$ compositions, and classified as A-type and within-plate granites (Text fig. 3). The charnockite and anorthosite-ferrodiorite rocks crystallised from dry magmas under reduced conditions, but the coexisting hornblende-bearing A-type granitoids were formed under oxidised conditions during the same melting episode (Duchesne *et al.* 2010), suggesting a coeval, but not comagmatic, origin of the AMCG suite.

Within this AMCG area (Text-fig. 2), about 15 km west of Bilwinowo IG-1 and the centre of the SAM, other opx-bearing rocks with slightly distinct geochemical characteristics have been recognised in the Łanowicze PIG-1 borehole section (Text fig. 3). The charnockites from the Łanowicze PIG-1 borehole section have previously been considered as components of the AMCG suite (Bagiński *et al.* 2001), but the evidence of deformational features such as foliation and the presence of garnet imply a distinct origin. P-T studies revealed that charnockites from the Łanowicze PIG-1 borehole section belong to the group of metamorphic rocks, partially formed under granulite-facies conditions (Bagiński *et al.* 2006).

## Charnockites from the Łanowicze PIG-1 borehole section

The Łanowicze PIG-1 borehole section provides insights into almost 600 m of crystalline rocks from a depth of 918 m to 1510 m typically containing orthopyroxene (opx). In the archival documentation of this borehole, the section was sub-divided into three rock groups (Text-fig. 4), differing from each other by textural features, mineral assemblage, or size of mineral grains. The simplified lithological log of the Łanowicze PIG-1 borehole consists of at least three main units, which in depth order are: (1) a unit of porphyric opx-bearing granodiorite with no foliation (918.0–985.7 m depth interval), which is interpreted as magmatic charnockite related to AMCG, (2) a unit of so-called granite-gneisses, usually opx-bearing (e.g., charnockite gneiss), with foliation (985.7–1391.0 m depth interval), and (3) a unit, in which granulites dominate (1391.0–1510.0 m depth interval). The granite-gneiss unit is cross-cut by pegmatite and fine-grained granite veins at 1107–1108 m, 1143–1146 m, 1224–1225 m, and 1367–1372 m depth intervals. Furthermore, a tectonic zone with breccia occurs in the 1027–1046 m depth interval. These document the tectonic complexity of the main opx-bearing granite-gneiss unit. The typical mineral assemblage of each unit is nominally anhydrous, containing opx.

The granulite unit (1391–1510 m depth interval) is characterised by the coexistence of K-feldspar, quartz,

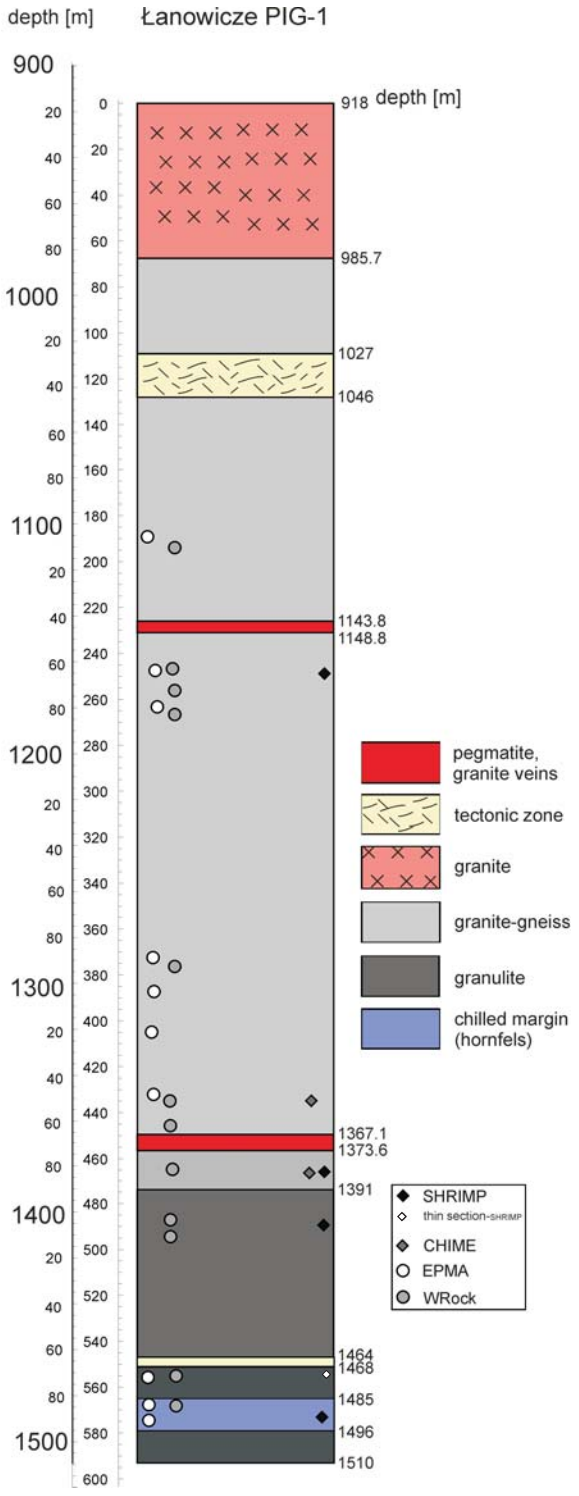


Text-fig. 4. Generalised lithological log of the Łanowicze PIG-1 borehole, total depth of 1510 m, including crystalline part with a total thickness of only ~592 m according to the archival written record (scale in metres). Locations of samples for U-Pb dating and CHIME dating (Bagiński 2006), whole-rock geochemistry and EPMA mineral chemistry are shown

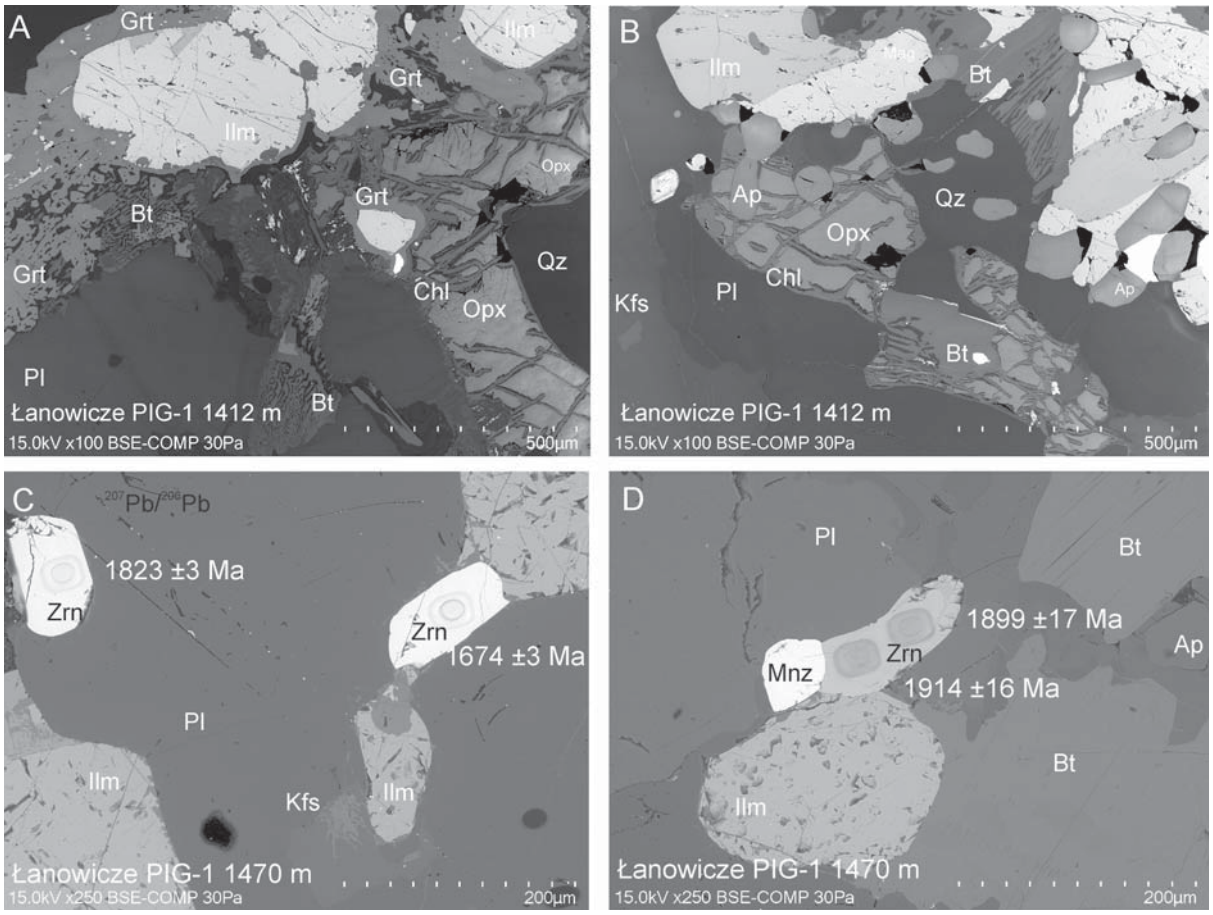


Text-fig. 5. Representative back-scattered electron (BSE) images showing the main mineral assemblage of the Łanowicze PIG-1 borehole charnockite. **A** – garnet-biotite pair and orthopyroxene; orthopyroxene-biotite and accessories; **B** – garnet-biotite pair and accessories; **C** – zircon grains between ilmenite; **D** – zircon and monazite. Pits after SHRIMP analyses on thin section with Pb-Pb ages are presented. Mineral abbreviations after Whitney and Evans (2010)

plagioclase, biotite, garnet, orthopyroxene and ilmenite, regarded as a stable mineral assemblage during high-grade metamorphism. The grain boundaries are marked by corona textures representing the metamorphic growth of garnet. The symplectitic intergrowth of two or three phases may be observed (Text-fig. 5A, B). Apatite, zircon, monazite and Fe-Ti oxides occur as the main accessory minerals (Text-fig. 5C, D). At the 1485–1496 m depth interval (termination of the drilled section), a chilled margin was recognised. Rocks within this chilled margin are more fine-grained than the others, and thus were described also as hornfelses. It was interpreted as a possible contact zone with the intruding anorthosite massif.

Orthopyroxene (opx) remains the most important mineral phase for charnockite rocks. The major element contents of opx from granite gneiss (e.g., charnockite gneiss) and granulite units, revealed that opx has a limited compositional variation along the Łanowicze PIG-1 borehole section (Text-fig. 6A). According to Morimoto's (1988) pyroxene nomenclature, the opx from both units can be classified as ferrositite. The CaO content is low (< 0.2 wt. %). The Mg-number Mg#/[$Mg^{2+}$ /$Mg^{2+}$ +$Fe^{2+}$] of opx in the granite-gneiss unit ranges at 0.43–0.46, and for opx from the granulite unit Mg#/ is only slightly lower, ranging at 0.41–0.44. Some of the charnockites studied have opx with an elevated content of $Al_2O_3$ (> 3 wt. %). The $X_{Al}$ usually ranges at 0.13–0.15 atoms per formula unit [a.p.f.u.], calculated on the basis of 6 oxygens, but in the case of samples from depths 1323 m and 1508 m, higher $X_{Al}$ values ranging at 0.20–0.17 are documented for opx (Text-fig. 6B). The predominantly euhedral shapes of opx crystals are consistent with their magmatic crystallisation. The mechanism of $Al_2O_3$ enrichment of opx (2.8–4.5%) could be related

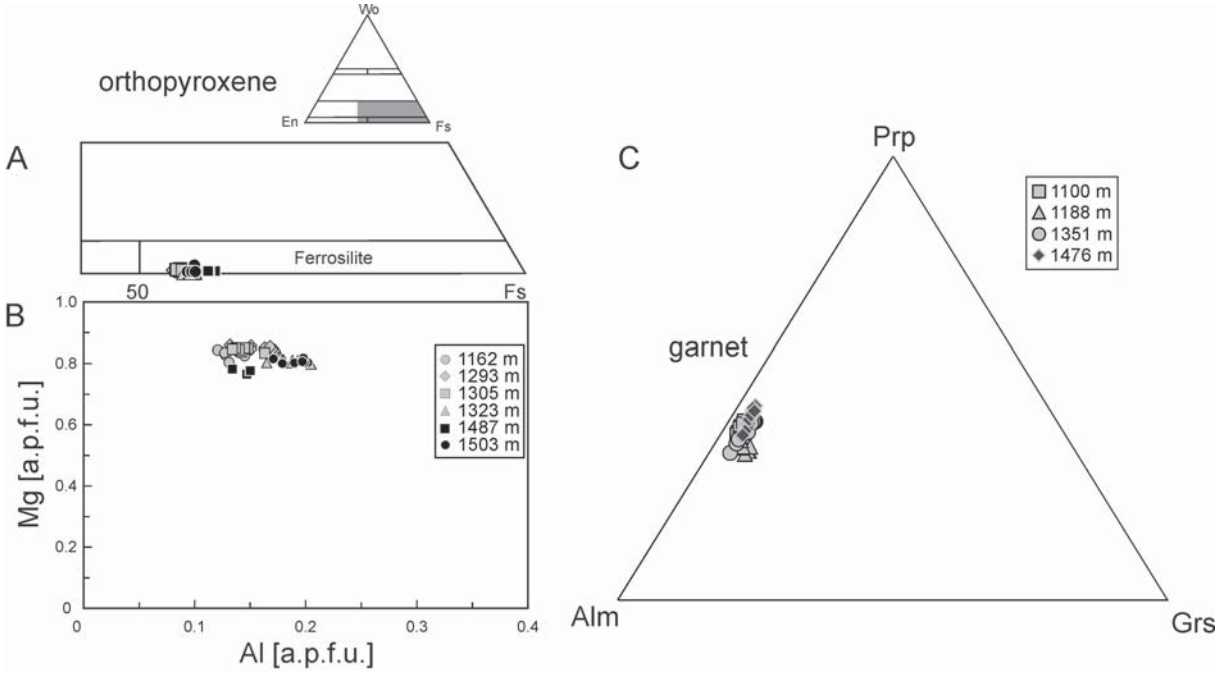


Text-fig. 6. A – Composition of orthopyroxenes on the Wo-En-Fs diagram (Morimoto *et al*. 1988). All pyroxenes are ferrosilite in composition. B – Mg a.p.f.u. variation in orthopyroxenes against Al a.p.f.u. content. C – triangular plot showing chemical composition of garnet from granite-gneiss and granulite samples of the Łanowicze PIG-1 borehole section. Symbols refer to samples collected from given depths

with early, relatively higher pressure crystallisation (> 5 kbar), taking place at greater depths.

Part of the biotite-rimmed opx crystals in charnockite have experienced partial alteration (Text-fig. 5A, B), which could indicate partial breakdown of primary magmatic opx outside its stability field at low temperatures.

Plagioclase crystals in the Łanowicze PIG-1 borehole section have an average anorthite content of ~0.46 in the core and ~0.40 in the rim. They usually show antiperthitic texture. Archival petrographic descriptions indicate that garnet (grt) was a characteristic mineral phase in the granulite unit, however it was also locally recognised in the upper part of the granite-gneiss unit. The contact between the adjacent grt-bearing and grt-absent portions is gradational. The grt occurring in granite-gneiss and granulite units is always relatively rich in the almandine component (about 60 to 80%) and pyrope (around 11–19%) with low (3–8%) grossular and spessartite end-members. The crystals from various depths show no significant differences of chemical composition (Text-fig. 6C).

Biotite occurs in the matrix and is associated with orthopyroxene, due to which we regard the mineral as a prograde/peak phase, although biotite is often regarded as a retrograde mineral in charnockite. In the charnockite rocks from the Łanowicze PIG-1 borehole, biotites from different depths have a high Ti content in range of 0.62–0.78 a.p.f.u. and a high *X*Mg value usually > 0.44.

The geothermometry of charnockitic rocks from various depths of both units, based on the garnet-biotite thermometer (Grt-Bt) of the Ferry and Spear (1978) formula, has documented a range of temperatures from a peak at 805ºC to retrogression at 515ºC (Bagiński *et al.* 2006), but the most frequent results from the granite-gneiss unit (depth intervals 1162.5 m, 1293 m and 1351 m) indicate a temperature range of 764–712ºC and from the granulite unit (depth intervals 1476 m and 1487 m) a temperature range of 796–762ºC. The formula of Ti-in-biotite thermometer of Henry *et al.* (2005) has been applied to biotite from rocks of the granite-gneiss and granulite units. These calculated temperatures match the temperatures determined using Grt-Bt thermometry.

Melt inclusion studies in samples coming from the granite-gneiss unit (depth intervals 1070 m, 1102 m and 1188 m) have indicated temperatures of homogenisation in the range of 870–940ºC, 895–960ºC and 890–955ºC, which are much higher than the re-

sults calculated from Gr-Bt and Bt geothermometers (Bagiński *et al*. 2006). The melt inclusions occur in feldspar only and comprise mainly the dense $CO_2$ fluid phase, which is typical for many charnockites, where the $CO_2$ is responsible for the low $H_2O$ activity that is required for the stabilization of opx. Melt inclusions as evidence of the existence of a melt phase may suggest a magmatic origin of this charnockite suite (Touret and Huizenga 2012).

**Age evidence from the Łanowicze PIG-1 borehole charnockites**

The first geochronological record of the Łanowicze PIG-1 borehole charnockite rocks was provided by one sample from the middle part of section at a depth of 1381 m, on the basis of chemical monazite dating using in situ U-Th/Pb $_{total}$ with thin section methodology (Bagiński 2006). Different contents of Th, U, and Pb $_{total}$ in the monazite grains hosted by charnockite at 1381 m showed at least two events in their history: an older Palaeoproterozoic at 1785±40 Ma and a younger Mesoproterozoic at 1445±35 Ma (Bagiński 2006). Similarly, data from the 1354 m depth interval confirmed two distinct records of thermal events related with monazite formation at ~1820±30 and ~1540±30 Ma (unpublished data). There is also one SIMS result (unpublished data), where zircon grains yielded an age of 1805±16 Ma (NORDSIM), that tentatively suggested a distinct origin of opx-bearing rocks in the Łanowicze PIG-1 borehole, with no relationship to the charnockitic members of the Mazury AMCG suite.

## MATERIAL STUDIED

This geochronological project was specifically targeted to determine the timing of protolith formation and metamorphic events in the Łanowicze PIG-1 borehole, located within part of a basement, which is the domain of a Mesoproterozoic AMCG suite.

The samples for geochronology were selected from the granite-gneiss and granulite units, as their lithology was interpreted to have been formed during high-grade metamorphism and reflects pre-existing deeper crustal host rocks.

Zircon was separated from four samples collected from the depth intervals of 1162 m and 1381.6 m for the granite-gneiss unit, and 1405 m and 1485 m for the granulite unit, an about 323 m thick charnockite interval being most representative of the Łanowicze PIG-1 borehole section (Text-fig. 4). One of the samples derives from the same core interval (1381 m), in which monazite chemical dating was performed. Each sample has also its whole-rock characteristics (Suppl. Table 1). They have tonalite (1162 m) and granodiorite compositions (1385 m, 1405 m, 1485 m), with $SiO_2$ contents from 63.13 wt. % (1162 m) to 69.87 wt. % (1485 m), and Zr contents from 349 ppm (1162 m) to 232 ppm (1405 m). All rocks are orthopyroxene-bearing, consisting also of quartz, plagioclase, K-feldspar, biotite, zircon, apatite, monazite and Fe-Ti oxides, and commonly minor garnet grains.

## ANALYTICAL METHODS

A U-Pb isotope age investigation was conducted using the SIMS (Secondary Ion Mass Spectrometry) technique on Sensitive High Resolution Ion Microprobe SHRIMP II. The measurements were performed on two different instruments: SHRIMP II, at Geoscience Australia in Canberra (sample Łan-1405) and SHRIMP IIe/MC at the Polish Geological Institute-National Research Institute in Warsaw (samples Łan-1162, Łan-1381.6, Łan-1485).

Similar sample preparation procedures, analytical setups for ion microprobes and data treatment according to the canonical description of Williams (1998) have been applied during work in both SHRIMP labs.

Zircons were separated from rock samples and concentrated by crushing, Frantz electromagnetic separation machine, heavy liquids, and handpicking. Zircons were mounted in 25 mm diameter epoxy discs together with the U-concentration standard SL13 (238 ppm U), the U-Pb standard TEMORA-2 (416.8±0.3 Ma; Black *et al*. 2004), and the $^{207}Pb/^{206}Pb$ standard OG1 (3465.4±0.6 Ma; Stern *et al.* 2009). The images of reflected and transmitted light and cathodoluminescence (CL) recognition were used to decipher internal growth phases of the grains.

Both SHRIMP instruments used focusing of an $O^{2-}$ ion beam to perform *in situ* U-Th-Pb isotope analyses with a spot size of 20–23 μm on sectioned zircon during an analysis time of about 15 min.

One spot on the standard zircon Temora2 was analysed after every three analyses of unknown zircons. The U-Pb data reduction was done using SQUID2 Microsoft Excel macro (Ludwig 2009). All isotopic ratios were corrected for common Pb on the basis of measured $^{204}Pb$. Tera-Wasserburg (1972) concordia plots and weighted mean $^{207}Pb/^{206}Pb$ ages were calculated by ISOPLOT/EX (Ludwig 2004) and the mean square of the weighted deviates MSWD is always shown. Final ages quoted in the text are at $2\sigma$ error,

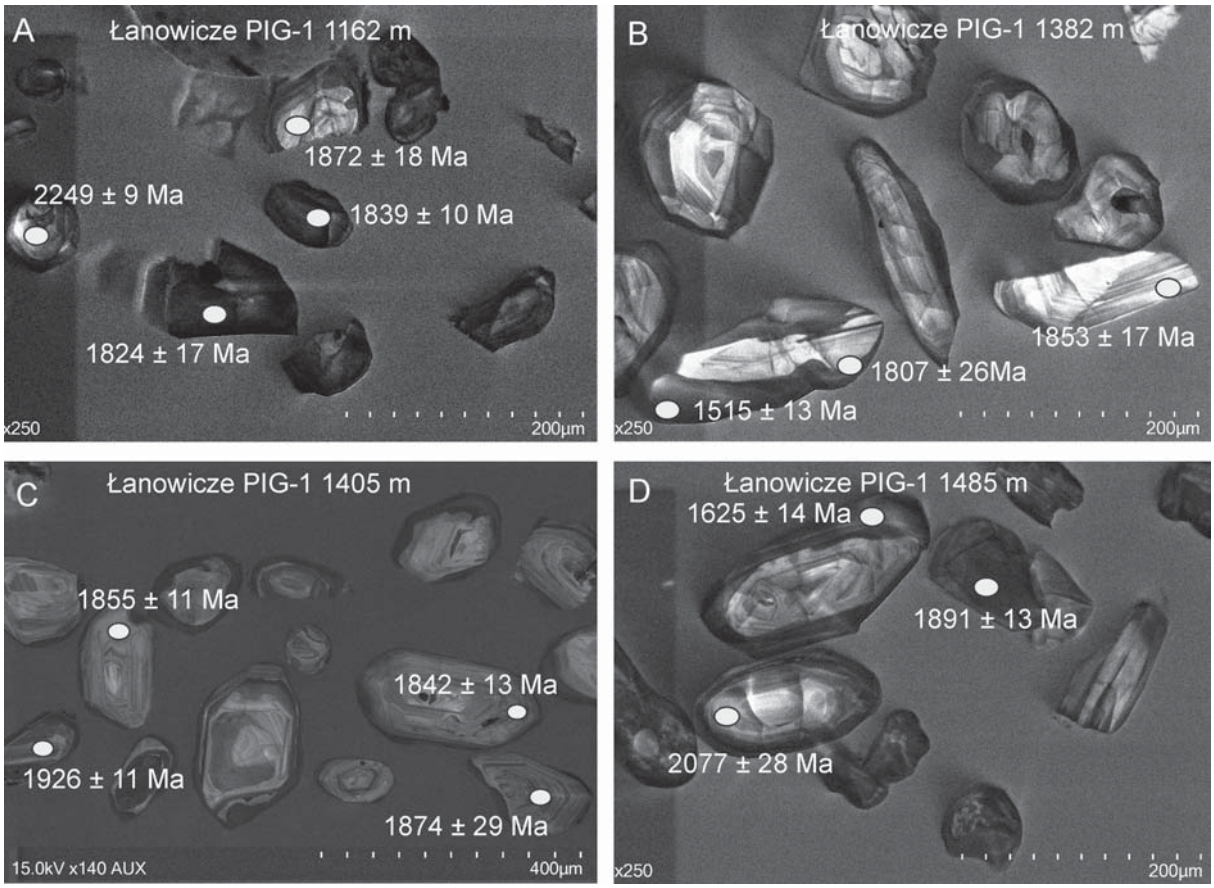


Text-fig. 7. CL-images of zircons, with complex internal textures, from high-grade charnockitic rocks of the Łanowicze PIG-1 borehole section, depths: A – 1162 m; B – 1382 m; C – 1405 m; D – 1485 m. Spots of SHRIMP analyses with Pb-Pb age results are marked

whereas those (single spot) in the tables of analytical results are reported at 1$\sigma$ error. During data reduction, only analyses, defined as less than 10% discordance (% disc. = [1–($^{206}$Pb/$^{238}$U age)/($^{207}$Pb/$^{206}$Pb age)] × 100) were considered in the age evaluation (% discordance; Suppl. Table 2) and the calculation of pooled ages, which is more commonly used as the generally accepted filter (Spencer *et al.* 2016).

U-Pb dates have been also acquired in one thin section (from 1470 m) as a test (Text-fig. 5C, D). A limited number of zircon grains provided a non-representative dataset for the sample, therefore they are not recommended during the age study. They were used for general considerations about the age of the charnockite suite formation.

The chemical composition of minerals used for this contribution has been analysed in thin sections using a Cameca SX 100 electron microprobe (Inter-Institutional Laboratory, Faculty of Geology, University of Warsaw) and BSE imaging was performed on Hitachi SU 3500 device at PGI-NRI in Warsaw.

## RESULTS

### Whole-rock geochemistry

Whole-rock analyses were made at the ACME Laboratory using XRF and ICP-MS methods (Suppl. Table 1) on the orthopyroxene-bearing rocks sampled in depth intervals of 1111.5 m and 1485.0 m, which include the granite-gneiss unit (8 analyses) and the granulite unit (5 analyses). They mostly represent intermediate to silicic composition with $SiO_2$ in the range of 57–69 wt. % (Suppl. Table 1). They can be classified mostly as granodiorite with only a few tonalites *sensu* R1-R2 classification of De la Roche *et al.* (1980). The $K_2O/Na_2O$ ratio is typically > 1. These rocks reveal a transition between metaluminous and slightly per-

aluminous affinities (Text-fig. 3), with Aluminum Saturation Indexes ($Al_2O_3/K_2O+Na_2O+CaO$) from 0.9 to 1.1, in contrast to metaluminous characteristics of A-type granitoids of the AMCG suite. The rocks from the Łanowicze PIG-1 borehole section display calc-alkaline and magnesian (Mg# = 34–39) features. The analyses reveal significant to low negative Eu anomalies (Eu/Eu* = 0.18–0.91) and low to moderate degrees of REE fractionation $[La/Yb]_N$ = 10–67. Geochemically, the rocks from both units differ only slightly.

The highest ΣREE content was found in samples from the granite-gneiss unit (259–799 ppm). The granulite unit exhibited (Suppl. Table 1) lower and more uniform ΣREE concentrations (229–320 ppm).

Similarly, the content of Zr is higher (203–514 ppm) in samples from the granite-gneiss unit in comparison to those from the granulite unit (199–325.8 ppm). The diagnostic sum of Zr+Nb+Ce+Y is high (339–598 ppm), falling on the border and within the field of A-type granites (Whalen *et al.* 1987). They form a continuous group with an affinity to both S- and A-type granitoids and straddle the line between areas shown as volcanic arc granites (VAG) and within-plate granites (WPG), suggesting a complex evolution or/and a transition from arc-like to post-collisional geochemical features of the protolith.

**Single zircon geochronology**

The set of zircon grains from the Łanowicze PIG-1 borehole samples, where a long and multiphase tectono-metamorphic history was expected, do not consist of homogeneous crystals like most grains derived from the AMCG, but contain numerous components, such as old inherited cores surrounded by magmatic or metamorphic overgrowths.

Zircons from the Łanowicze PIG-1 borehole samples are either euhedral prismatic grains or broken prisms with most of them being from 150 to 200 μm in length. SEM CL imaging revealed the true complexity of the internal structures. The zircon grains always have an internal core and metamorphic rim, which is consistent with the metamorphic evolution of the Łanowicze PIG-1 borehole charnockite rocks (Text-fig. 7). The metamorphic overgrowths are texturally distinct, represented by thin domains (< 20 μm) of weak luminescence (dark grey).

The cores are interpreted as representing mostly an igneous origin formed during the magmatic crystallisation of the protolith. A significant component shows oscillatory zoning but in many cases, the internal parts of the grains have more irregular CL images. Moreover, evidence of crystal-plastic deformation of zircon is common in samples Łan-1382 and Łan-1485. They were formed before the stage of metamorphic overgrowth formation. These deformation features or even microcracks limit the selection of proper grains or spots for the analysis. Some of the magmatic origin cores exhibit recrystallisation symptoms as shown by darker grey zones that overprint the magmatic zonation. Recrystallisation usually affected only the outer domains of the cores.

The results of all U-Pb zircon isotopic analyses were merged and shown in Suppl. Table 2. The U-Pb zircon analyses of the Łanowicze PIG-1 borehole samples contain a mix of concordant to slightly discordant data.

*Sample Łan-1162*

Eighteen zircons were analysed. Nearly all the cores yield a $^{207}Pb/^{206}Pb$ age in the range of 1872±18 to 1795±8 Ma. Only one older core recorded an age of 2249±9 Ma. A single measurement within a rim documents metamorphic crystallisation (Th/U < 0.1) at 1583±12 Ma. The main group of data (Text-fig. 8A, B) is concordant (discordia ±4%) and n = 12 spots gave a concordia age of 1836.6±7.4 Ma (MSWD = 0.18). For comparison, the weighted mean $^{207}Pb/^{206}Pb$ age from n = 14 spots is 1837.2±8.4 Ma (95% confidence limits and MSWD = 1.6).

*Sample Łan-1381*

Because of the complexity of zircon internal features in this sample, 48 spots collected from 47 different zircon grains were analysed. Two analyses have been rejected (including an older one of 1922±44 Ma) due to more than 10% discordance. The remaining 46 (< 10% discordant) range from 1898±38 to 1721±17 Ma. Only one single spot documents an age of metamorphic overgrowth at 1515±13 Ma. A relatively uniform age group of 18 grains (Text-fig. 9A, B) defines a concordia age of 1849.9±9 Ma (MSWD = 5.9). The selection of a few youngest analyses from internal overgrowths with low luminescence allowed us to extract 4 grains with a lower intercept concordia diagram of 1799.7±24 Ma (MSWD = 0.32).

*Sample Łan-1405*

Twenty seven zircon analyses were collected from 27 zircons. All analyses are nearly concordant (discordance < 5%) and contain < 0.2% common $Pb_c$. One of the spots located within the outer part of a grain

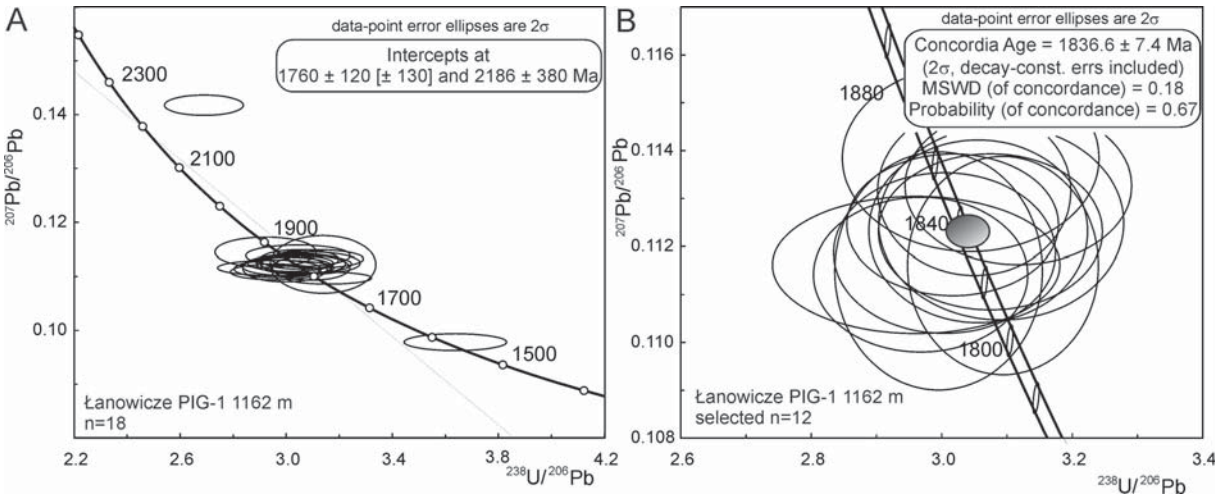


Text-fig. 8. Tera-Wasserburg concordia diagrams showing results of zircon analyses from the Łanowicze PIG-1 borehole section, sample depth 1162 m (Łan-1162): A – all data collection, including inheritance and metamorphic zircon domains; B – zircon dominant cluster extracted

yielded a crystallisation close to metamorphic (Th/U = 0.18) at 1653±13 Ma. Another shows an inherited core with an age of 1926±4 Ma. The remaining 25 analyses range from 1874±29 to 1776±16 Ma. Most (20 analyses) define a concordia age (Text-fig. 10A, B) at 1842.3±6.4 Ma (MSWD = 0.81). The same age group yielded a weighted mean $^{207}Pb/^{206}Pb$ age of 1844.2±5 Ma (95% confidence; MSWD = 0.62; probability of fit = 0.90). Another four spots from the rim and relatively outer part of a zircon yielded a concordia age of 1799±10 Ma (MSWD = 0.13).

*Sample Łan-1485*

A total of 50 zircon analyses from 44 grains were made, where 6 grains provided data from both rim and core area. The rim results are discordant with a discordance of 8–20%, thus only a group of 4 zircon grains was considered to constrain the age of metamorphic overgrowth.

The single spot ages from cores also are more discordant (Suppl. Table 2) than the results obtained from other samples. Data reduction was prepared on selected n = 31 concordant or nearly concordant analyses (discordance < 10%). They form at least two to three apparent groups (Text-fig. 11A) of 8 core results in the range of 2270±31 to 1904±14 Ma, 20 grains in the range of 1888±12 to 1830±8 Ma, and 3 grains from 1764±12 to 1611±18 Ma (Pb-Pb). The main group defined a lower intercept at 1839±100 Ma (MSWD = 0.0119).

The age of crystallisation constrained for most concordant cores of this group was at 1881±16 Ma (Text-fig. 11C).

*Sample Łan-1470 – thin section*

Only six zircon crystals were found in this thin section from the depth of 1470 m. This is quite a limited number for such a complex case, thus it is treated as approximate information only. Seven spots were analysed in a thin section mode. The Pb-Pb age of crystallisation for these grains was obtained at 1647±18, 1674±3, 1783±6, 1823±3, and 1841±3 Ma, and within one zircon core at 1899±16 and 1914±16 Ma (Text-figs 5D and 11D), confirming the time-frame obtained on single grain collection from adjacent depths (e.g., 1405–1485 m).

## DISCUSSION

The complexity of internal textures of zircon grains from the Łanowicze PIG-1 borehole charnockite suite (1162–1485 m depth interval), reflects the composite history of their formation. The protolith of these rocks was affected by more than one metamorphic event, including high-grade conditions. Compared to the temperature of metamorphism deciphered from the granite-gneiss unit (764–712ºC), the granulite unit was metamorphosed at slightly higher temperatures (796–762ºC) and some of them also at slightly higher pressures (elevated contents of $Al_2O_3$ in opx). Interpretation of

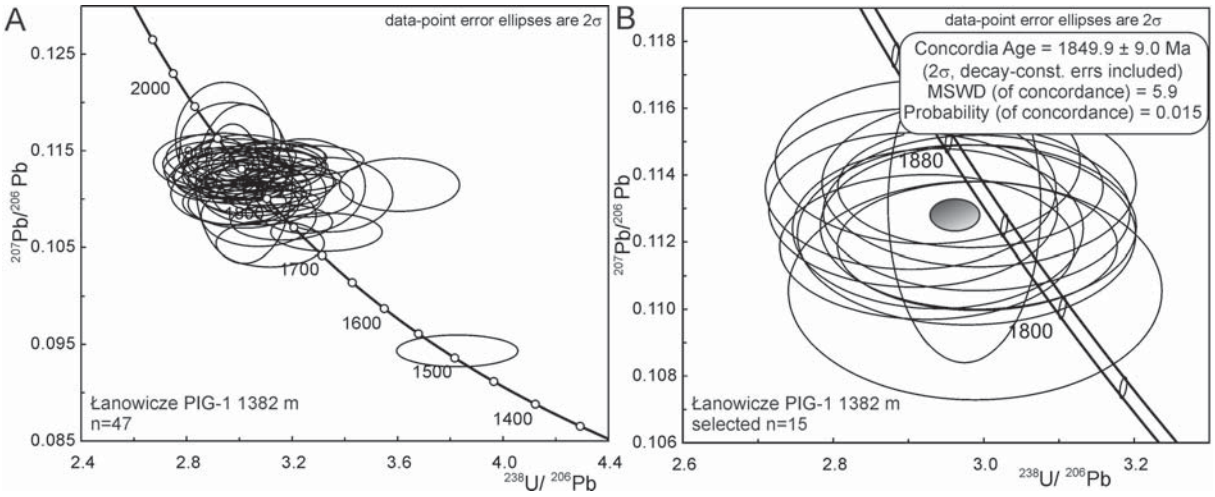


Text-fig. 9. Tera-Wasserburg concordia diagrams showing results of zircon analyses from the Łanowicze PIG-1 borehole section, sample depth 1386 m: A – all data collection, including metamorphic rim; B – zircon dominant cluster extracted

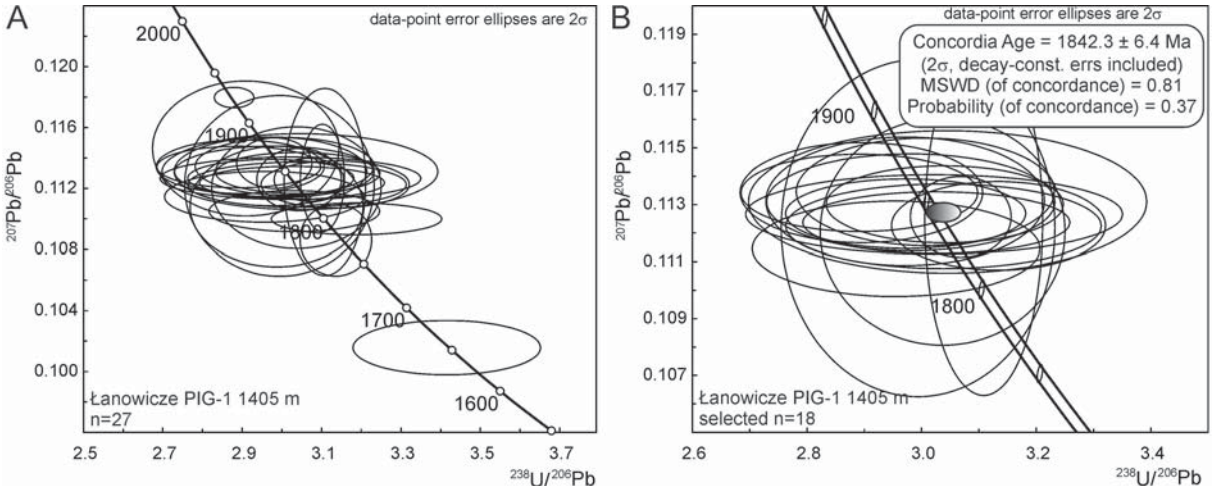


Text-fig. 10. Tera-Wasserburg concordia diagrams showing results of zircon analyses from the Łanowicze PIG-1 borehole section, sample depth 1405 m: A – all data collection, including inheritance and metamorphic zircon domains; B – zircon dominant cluster extracted

the age results obtained from high-grade metamorphic rocks requires a lot of attention, because of the different response of the U-Pb system to particular conditions, such as an absence *versus* presence of fluids in the system and the duration of high-grade conditions (Kröner *et al.* 2014). Moreover, the irregular distribution of the garnet in the granulite unit of the Łanowicze PIG-1 borehole section seems to be a significant factor during possible zircon-forming reactions, particularly during the retrograde replacement of garnet by other mineral phases, when new zircon may grow as a result of Zr-liberating reactions of garnet breakdown (Harley *et al.* 2007; Kohn *et al.* 2015; Rubatto 2017).

**Metamorphic episodes**

A common criterion of discriminating between magmatic *versus* metamorphic zircon remains is the Th/U ratio (Hoskin and Black 2000; Rubatto 2002), where Th/U < 0.1 usually indicates a metamorphic origin, whereas Th/U > 0.1 suggests a typical magmatic origin. However, for high (and particularly ultra high) temperature samples, the Th/U ratio should

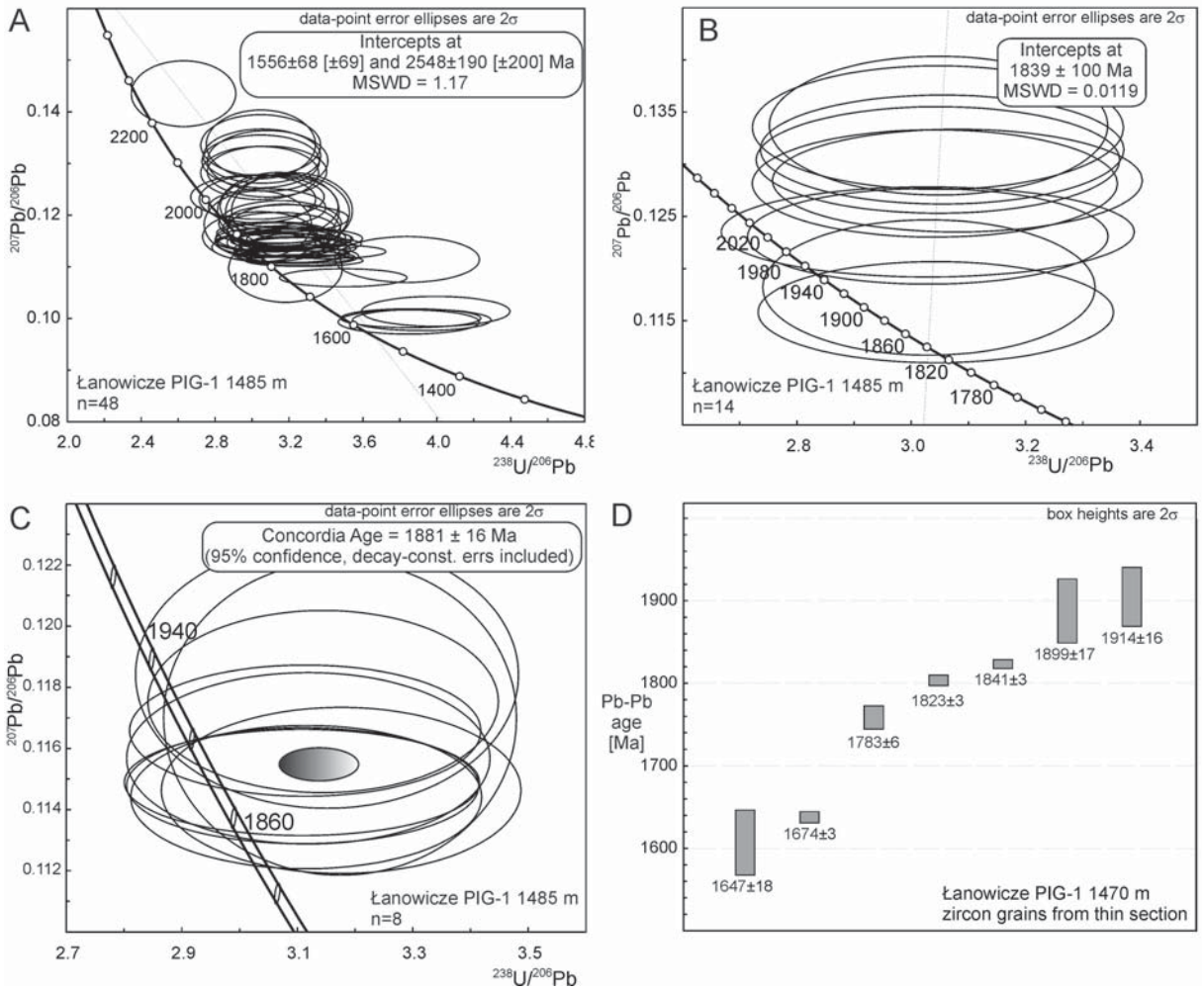


Text-fig. 11. Tera-Wasserburg concordia diagrams showing results of zircon analyses from the Łanowicze PIG-1 borehole section, sample depth 1485 m: A – all data collection; note variation and discordance of isotopic composition; B – zircon dominant cluster extracted

be used with caution, especially when the accompanying accessory phase was monazite (Harley *et al*. 2007; Rubatto 2017). In such a case, concentrations of Th and U in zircon were influenced by the partitioning behaviour of Th and U between zircon and co-existing monazite.

Taking into account the zircon grains collection from the Łanowicze PIG-1 borehole, the record of metamorphic stages was deciphered from the "topography" of grains, e.g., from various overgrowths and inner domains with weak zoning (documented by CL), because high-grade metamorphic zircon often displays a relatively low CL emission (Rubatto 2017).

The youngest episode is represented by weak rims that surround some grains, with low Th/U < 0.1 (Text-fig. 7B). These rims are usually thinner than ~20 μm, thus only a few measurements have been made (Text-figs 9 and 10). Data from samples Łan-1381 and Łan-1485 reflect metamorphic events at 1514±13 and 1516±28 Ma, respectively. They have a poor precision because of the discordance exceeding 10%, but in general they correspond to the time of the AMCG suite emplacement known from the Boksze IG and Filipów IG-1 borehole samples at 1512±1 Ma (Dörr *et al*. 2001) and at 1512±17 Ma (Wiszniewska *et al*. 2016), respectively. At the same time, amphibolite facies metamorphism was marked along E–W-trending lineaments in central and south-eastern Lithuania (Skridalite *et al*. 2008).

Evidence of slightly older metamorphic domains that crystallised at 1583±12 Ma was recognised in sample Łan-1162. This event in the range 1.62–

1.58 Ga was documented by the chemical ages of the monazite population derived from the WL (Skridlaite *et al*. 2014).

Zircon grains from samples Łan-1381 and Łan-1405 display also inner domains that form low luminescence areas with crystallisation ages at 1799±24 and 1799±10 Ma, respectively. This high-grade metamorphic episode was frequently noted (Bogdanova *et al*. 2006, 2015) by the age study from the late Palaeoproterozoic belts extending between the south of Estonia, Lithuania (WL) and Belarus (BPG), including U-Pb zircon dating of the WL metamorphism documented at 1796±2 Ma (Claesson *et al.* 2001) and the peak of granulite facies condition in PBG obtained at 1790±8 Ma (Bibikova *et al*. 1995). In general, it was the time of major aggregation of the EEC (Skridalite *et al.* 2009).

In the Łanowicze PIG-1 borehole the zircon internal domains with weak luminescence, e.g., with relatively low CL emission typical of high-grade metamorphic zircon, were formed between 1.79–1.80 Ga. In terms of tectonic criteria it was a post-collisional (1.8 Ga) stage, marked also by the emplacement of numerous ultramafic, mafic and granitic rocks in the Fennoscandia/Sarmatia borderline, in response to collision of both blocks (Bogdanova *et al.* 2013; Shumlyanskyy *et al.* 2016). It is very probable that such significant thermal event at about 1.80 Ga corresponding to the peak of dry metamorphism affected the charnockite rocks from the Łanowicze PIG-1 borehole, from depths over 918 m. In the absence of fluids, when the metamorphism is dry, the new zircon domains may grow *via* solid-state (partial) recrystallisation (e.g., Hoskin and Black 2000; Kuntz *et al*. 2018) or/and by the breakdown of Zr-rich minerals. A few phases in charnockite rocks, particularly coexistence of garnet or pyroxene and ilmenite, contain a ppm range concentration of Zr that increases exponentially with temperature (Bingen *et al.* 2001; Kohn and Kelly 2018). The textural relationships (Text-fig. 5C, D) do not always demonstrate just a reaction on the grain boundaries, but if such a mineral assemblage occurs, the development of new zircon zones remains possible even during dry metamorphic conditions. Thus, the presence of garnet and ilmenite in the Łanowicze PIG-1 borehole high-grade rocks effectively favours metamorphic zircon growth in a dry regime.

**Protolith age**

The majority of U-Pb zircon absolute age determinations for the Łanowicze PIG-1 borehole charnockites were collected to identify the age of the protolith of these rocks. They were, however, affected by granulite facies metamorphism that has been recognised previously by petrographic studies (Bagiński and Krzemińska 2004). The high mean value of the closure temperature for the U-Pb system in zircons, in consequence of the exceedingly slow diffusion rates in pristine/crystalline zircon, means that 'blocking' or 'closure' temperatures lie outside the realm of crustal metamorphism in the range > 950–1000ºC (Cherniak and Watson 2000). Thus, zircons from high-grade rocks usually preserve the time of crystallisation of the igneous protolith, but opposite examples of partial resetting of the U-Th-Pb isotopic system might be common during high-grade metamorphism (Wan *et al.* 2011 and references therein), leading to the scattered distribution of analyses near the concordia curve. Fortunately, most U-Pb core results from the Łanowicze PIG-1 borehole (Text-figs 8A, 9A and 10A) remain concordant or nearly concordant. They demonstrate a few distinctive clusters on the concordia diagrams. In the case of sample Łan-1162, about 78% of the data (14 of 18 spots analysed) are grouped together, giving the concordia age of 1835.9±7 Ma. Such a uniform cluster most likely reflects the age of the igneous protolith.

Sample Łan-1381 shows more dispersed values of U-Pb isotope ratios (Text-fig. 9A), which is probably related to the plastic deformation widespread in the zircon cores formed mostly before metamorphic overgrowths. This plastic deformation in the zircon crystal lattice potentially acts as fast diffusion pathways facilitating Pb, U and Th migration (Kovaleva et al 2014).

It was possible, however, to select even 39% of the grains (18 of 46 spots analysed) that provided a crystallisation age of 1849.9±9 Ma (concordia age). Several older, probably inherited zircon cores were also noted in this sample.

A very similar age of the protolith was determined at 1405 m (Text-fig. 10A). About 79% of the zircons (20 of 27 spots analysed) reveal comparable isotope ratios with a concordia age at 1842.3±6.4 Ma. These ages were obtained from zircons with undisturbed igneous zonation from undeformed cores and thus are thought to date igneous crystallisation.

Coherent ages within the error range: 1837±7, 1850±9, and 1842±6 Ma (and ~1841±3 Ma repeated in the thin section) deciphered for three samples, *viz*. Łan-1162, Łan-1385, and Łan-1405 (and thin section depth 1470 m), seem to be coeval with the magmatic episode widespread in the Lithuanian basement. The MLD consists predominantly of magmatic rocks (Motuza 2005; Motuza *et al.* 2008; Skridlaite

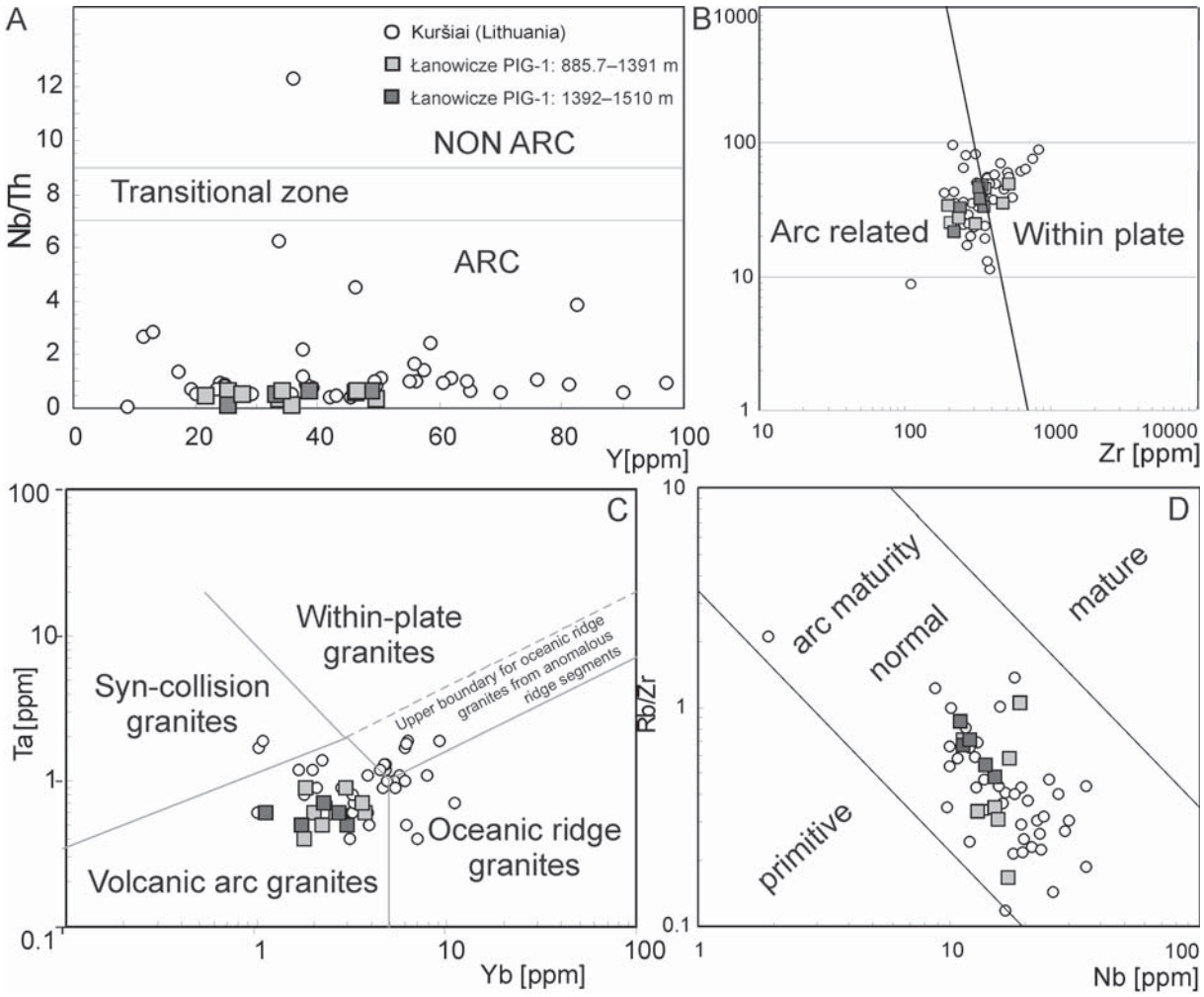


Text-fig. 12. Geochemical tectonic discrimination diagrams comparing the Palaeoproterozoic charnockite suite of the Łanowicze PIG-1 borehole (this study) and the Kuršiai (WL) batholith (after Motuza *et al.* 2008). A – Nb/Th *vs* Y diagram (after Jenner *et al.* 1991); B – Y *vs* Zr diagram for arc-related and within-plate granites (after Müller and Groves 1997); C – Ta *vs* Yb tectonic discrimination diagram (after Pearce *et al.* 1984); D – Nb *vs* Rb/Zr arc maturity discrimination diagram (after Brown *et al.* 1984)

*et al*. 2011) that represent a once active continental margin. The northern and western parts of the MLD and WL margins comprise various charnockites and granulites. Their ages vary between c. 1.86 and 1.82 Ga. During this time, the charnockitic Kuršiai batholith was formed (Motuza *et al*. 2008; Motuza and Motuza 2011). The lithologies of the Kuršiai batholith ranged through intermediate and acidic varieties, with ferroan, calc-alkalic, peraluminous, and granite with straddle S- and A-type geochemical signatures (Motuza and Motuza 2011). Whole-rock compositions and geochemical data from the Łanowicze PIG-1 borehole suite (Suppl. Table 1) and the Kuršiai batholith were compared using several diagnostic plots (Text-fig. 12A–D). Trace element concentrations and discrimination diagrams suggest a volcanic arc setting. Rocks of the Kuršiai batholith and the Łanowicze PIG-1 borehole charnockites have consequently specific trace element characteristics similar to those of arc or arc-related volcanic arc granites (VAG) with normal maturity (*sensu* Brown *et al.* 1984; Pearce *et al.* 1984; Jenner *et al.* 1991; Müller and Groves 1997). Limited U-Pb zircon data from the Kuršiai batholith provided (discordant line with intercept) ages at 1844±5 (MSWD = 1.3), 1837±6, and 1846±12 Ma (Motuza *et al*. 2008).

A very similar age of magmatic crystallisation at 1839±15 Ma has been obtained recently (Bogdanova

*et al*. 2015) from the granulite of Geluva in Lithuania (MLD). Its mafic protolith was metamorphosed at about 1.80 Ga (upper intercept at 1809±9 Ma but weighted mean age of 1798±11 Ma). The MLD consists predominantly of magmatic rocks with an age of 1.86–1.84 Ga (Motuza 2005; Motuza *et al*. 2008; Skridlaite *et al*. 2011) that may possibly represent a once active continental margin (Bogdanova *et al*. 2015).

Somewhat older evidence from an area close to the MLD/LEL border are related to diorite bodies, intruded at 1859±5 and 1848±6 Ma in Zeimiai and Varlinis, respectively (Skridlaite *et al*. 2011). Zeimiai 347 and Varlinis 268 belong to the same prominent igneous Randamonys (gabbro-diorite-granodiorite) complex. The Łanowicze PIG-1 borehole suite was, however, metamorphosed in the granulite facies, whereas the south-eastern Lithuanian Randamonys complex was metamorphosed in the amphibolite facies, which is typical of the LEL domain (Skridlaite and Motuza 2001).

The results obtained from depth 1485 m demonstrate a problem of zircon discordance. The zircon cores, with crystal-plastic deformation that probably caused rapid diffusion of radiogenic Pb, are very characteristic for this sample (Text-fig. 7D). Plastic deformation of cores most likely occurred during the tectonic perturbation prior to metamorphism (the metamorphic overgrowths are not deformed). Usually, the sequence of tectonic events at active continental margins leads to complex deformation of the lithosphere, accompanied with metamorphism. Especially in subduction zones, in which the WL and MLD rocks occur together, a palaeo-subduction zone *sensu* Janutyte *et al.* (2015) is considered responsible for deformation and large-scale normal and strike-slip faulting.

Analyses of zircon, which have experienced isotopic disturbance after deformations, plot off the concordia line (Text-fig. 11A), forming a visual record of Pb exchange with the external environment by intra-grain Pb mobility (Pb loss). These discordant ages forming a discordia line with lower intercepts on the concordia diagram (but defined by zircons with a low U content < 100 ppm) were considered as a possible time of loss of a closed U-Pb system (Mezger and Krogstad 1997; Gehrels 2014; Schoene 2014; Reimink *et al*. 2016).

The lower intercept on the Łan-1485 concordia diagram (Text-fig. 11) clearly suggests a Pb-loss event at c. 1558±68 Ma. The depth interval of 1485–1500 m was strongly affected by an adjacent anorthosite igneous body of the SAM (the contact zone was reported to be a hornfels) intruded at 1.53–1.50 Ga.

Moreover, zircon core results, older than 1.9 Ga (Łan-1485), that form a cluster of about 30% of the analyses (15 out of 50 analysed) constrained a lower intercept age at 1839 Ma with poor precision of ±100 Ma (MSWD = 0.0119), but a selected group with relatively lower discordances (5–9%) and igneous zonation of cores yielded a concordia age of 1881±16 Ma (Text-fig. 11C), which is interpreted as the time of protolith crystallisation.

Rocks emplaced in a similar range of 1.88–1.89 Ga are widespread in the granulite domain of southern Estonia (e.g., SEG) as well as in northern Latvia and Lithuania (e.g., LEL). The nearest location of these rock types seems to be the garnet-bearing metadiorite (Lazdijai Lz8 borehole) of southern Lithuania situated almost 40 km to the north of the Łanowicze PIG-1 borehole. In this case, the crystallisation age of the igneous precursor was at 1887±2 Ma (Bogdanova *et al*. 2015). The Lz8 borehole granodiorite was formed in the lower crust (Skridlaite *et al*. 2003), but later was uplifted along a shear zone. It represents the LEL, which in that locality tectono-stratigraphically overlies the WLG.

There are a few more new age results in range of 1.89–1.87 Ga obtained in the LEL, beneath the Varena iron ore deposit (Siliauskas *et al.* 2018b). Four samples with calc-alkaline affinity from the LEL were selected for zircon U-Pb SIMS dating: two samples of granodiorite from the southern part of the LEL that might be part of the TTG suite, a sheared diorite and a meta-rhyolite from the western border of the LEL. The two granodiorites yielded concordia ages of 1892.3±5.7 (MSWD = 1.01) and 1893.7±7.4 Ma (MSWD = 1.9), whereas the diorite is somewhat younger at 1876.1±4.8 Ma (MSWD = 1.6) (Siliauskas *et al.* 2018b).

Other evidence is related with the calc-alkaline granodiorites of the southern part of Estonia, which yielded concordia ages of 1892.3±5.7 and 1893.7±7.4 Ma, and somewhat younger, diorite emplaced at 1876.1±4.8 Ma (Bogdanova *et al.* 2015 and references therein). There is also evidence of the garnet-orthopyroxene-cordierite-bearing granodiorite (SEG) with a magmatic crystallisation age of 1891±3 Ma (sample Kõnnu 300). These types of rocks originated from melts formed by high-temperature dry partial melting of mixed sources, probably comprising supracrustal rocks of various compositions (Bogdanova *et al.* 2015).

All these geochronological proofs collected between southern Estonia, northern Latvia and Lithuania (Text-fig. 13A) correspond with the overlapping, subsequent phases of the "semi-continuous" Svecofennian orogeny (Lahtinen *et al.* 2005) that

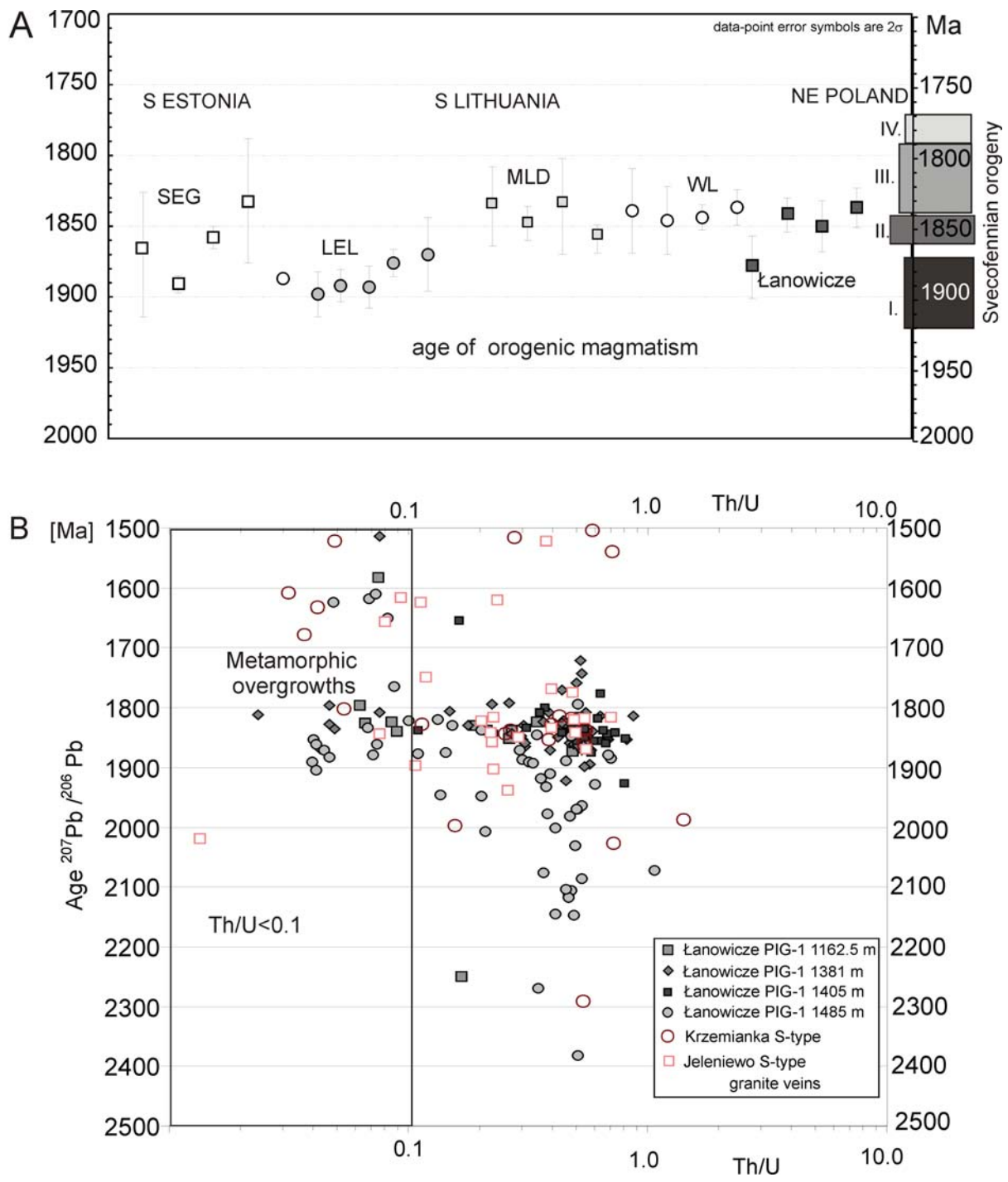


Text-fig. 13. A – Compilation of U-Pb documented magmatic orogenic events from the Baltic region, including data from the: South Estonian Granulite (SEG), Latvian-East Lithuanian domain (LEL), Mid-Lithuanian domain (MLD), West Lithuanian (WL) domain including the Kuršiai and Łanowicze PIG-1 charnockites. U-Pb zircon data from: Mansfeld (2001), Motuza *et al.* (2008), Skridlaite *et al.* (2011), Bogdanova *et al.* (2015), Siliauskas *et al*. (2018a, b) and this study. B – Plot of zircon single spot Pb-Pb age results *vs* Th/U ratio. Comparison of zircon grains from high-grade charnockite of the Łanowicze PIG-1 borehole with data from S-type granite veins from the group of Krzemianka and Jeleniewo boreholes in the area of AMCG (Wiszniewska and Krzemińska 2017). C – Simplified contour map of the Baltic countries and NE Poland with the location of the Łanowicze PIG-1 and Kuršiai charnockite samples and related rocks of the high-grade metamorphic regime from south Estonia. Phases of the Svecofennian orogeny after Lahtinen *et al.* (2005): (I) 1.92–1.87 Ga microcontinent accretion, (II) 1.86–1.84 Ga continent extension, (III) 1.84–1.79 Ga continent-continent collision, and (IV) 1.79–1.77 Ga orogenic collapse and stabilisation

comprise a stage of microcontinent accretion (1.92–1.87 Ga), continent extension (1.86–1.84 Ga), continent-continent collision (1.84–1.79 Ga), and orogenic collapse and stabilisation (1.79–1.77 Ga).

According to the view presented by Bogdanova *et al*. (2015) and Siliauskas *et al.* (2018a, b), the LEL was formed at c. 1.89 Ga in a volcanic arc environment mostly during the Svecofennian episode at 1.89–1.87 Ga, whereas the MLD is a new accretion on its margin that took place at ~1.86–1.84 Ga, when gabbros, diorites, granodiorites, and granites of the Randamonys complex intruded at c. 1.86–1.84 Ga (Rimsa *et al.* 2001; Skridlaite *et al.* 2011) within an Andean-type continental margin, followed by the younger c. 1.83 Ga episode (Bogdanova *et al*. 2015). These rocks, formed at 1.89 and 1.86–1.84 Ga within volcanic arcs, were later tectonically fragmented and metamorphosed at about 1.80 Ga. Finally, the pre-Mesoproterozoic basement was cross-cut by the c. 1.50 Ga anorogenic AMCG suite extending from Kabelai to the Mazury Complex.

Other remnants of Palaeoproterozoic crust in the area of the AMCG suite, but strongly reworked in the Mesoproterozoic, were recognised by the zircon study of the peraluminous granite veins and pegmatite cutting all AMCG components (Wiszniewska and Krzemińska 2017) and also noted in the Łanowicze PIG-1 borehole section. An important feature of these S-type granites emplaced between 1493–1489 Ma is the presence of a population of abundant inherited cores with ages mostly in the range of 2019±26 to 1815±10 Ma. The generation of peraluminous magma had to include the partial melting of the nearest surrounding crust. A simple comparison (Text-fig. 13B) of the core ages obtained from granite veins and the ages of the Łanowicze PIG-1 borehole protoliths exposed a series of similar projections in terms of age crystallisation and the Th/U parameter. All these pre-Mesoproterozoic age data accumulated from the vicinity of an AMCG undoubtedly reflect the main features of buried crust, existing prior to the formation of a within-plate AMCG suite. They also reflect the complexity of this part of basement (Text-fig. 13B). It was considered previously (Bogdanova *et al*. 2015) that the WL and the adjacent part of the MLD were over- thrust onto the LEL (Text-fig. 1) in few places. The significantly variable ages of the igneous protolith deciphered from the charnockite rocks of the Łanowicze PIG-1 borehole section, i.e., 1837±7, 1850±9, 1842±6 Ma *versus* 1881±16 Ma confirms this hypothesis. Such a complex zone occurring at an active continental margin records progressive subduction, accretion, addition of material to the upper plate, metamorphism, and exhumation, spanning the extended period of subduction.

## CONCLUDING REMARKS

The Łanowicze PIG-1 borehole section located within the AMCG Mazury Complex represents a unique relic of pre-Mesoproterozoic crust, formed at the active continent margin involved in a subduction stage. It provides insight into a series of events and processes:

The igneous activity is conspicuous in the Łanowicze PIG-1 borehole charnockite suite at 1836.5±7.4 (1162 m), 1849.9±9 (1382 m), 1842.3±6.4 (1405 m), and 1881±16 Ma (1485 m). Thus, the Łanowicze PIG-1 borehole contains components from both neighbouring tectonic domains MLD and WL, considered to represent a continental margin at 1.86–1.84 Ga formed during the middle Svecofennian orogenic phase and a fragmented LEL domain, where the oldest continental crust was generated at c. 1.89–1.87 Ga.

This composite suite of charnockites of igneous origin was deformed and tectonically dismembered during the subduction processes and affected by more than one metamorphic event, with a prominent for the area thermal phase at 1799±10 Ma interpreted as the peak of dry high-grade metamorphism, and then at 1583±12 Ma, which corresponds to the time of metamorphism at 1.62–1.58 Ga widespread within the WL.

The last thermal event was marked between 1514±13 to 1516±28 Ma, when the previously established continental crust was cross-cut by the Mesoproterozoic, c. 1.53–1.50 Ga, AMCG Mazury and Kabeliai Complex.

The zircon U-Pb age investigations completed by this contribution confirm that a fragmented LEL extends beneath the MLD and even WL up to northernmost Poland to the Łanowicze PIG-1 borehole area. The charnockite rocks studied, in which the opx preserved a relatively higher pressure crystallization (> 5 kbar) that took place at greater depths (~20 km), may also support this hypothesis.

**Acknowledgments**

Part of the U-Pb measurements reported here was carried out under the auspices of the collaborative research agreement between the Polish Geological Institute-National Research Institute (PGI-NRI) and the Australian Scientific Instruments (ASI) in Geoscience Australia (GA) Geochronological Laboratory. Other age data are from the M.Sc. project of Aleksandra

Łukawska performed at the Faculty of Geology, University of Warsaw (UW). Zircon separation was done by David DiBugnara at GA and Aleksandra Łukawska at UW. Geochemical data were collected during work on KBN project no. 3P04D 014 23, managed by Bogusław Bagiński. Raymond Macdonald is kindly acknowledged for his thoughtful reading of the manuscript. Thanks are extended to Mateusz Rechowicz for assistance with sample preparation at PGI-NRI and Zbigniew Czupyt for calibration of the SHRIMP analytical session at PGI-NRI. Grazina Skridlaite and an anonymous reviewer are thanked for insightful reviews that have greatly improved this paper.

## REFERENCES

Aranovich, L.Y. and Newton, R.C. 1995. Experimental determination of $CO_2$-$H_2O$ activity – composition relations at 600–1000ºC and 6–14 kbar by reversed decarbonation and dehydration reactions. *American Mineralogist*, **84**, 1319–1332.

Bagiński, B., Duchesne, J.-C., Vander Auwera, J., Martin, H. and Wiszniewska, J. 2001. Petrology and geochemistry of rapakivi type granites from crystalline basement of NE Poland. *Geological Quarterly*, **45**, 33–52.

Bagiński, B. and Krzemińska, E. 2004. Igneous charnockites and related rocks from the Bilwinowo borehole (NE Poland) – a component of AMCG suite – a geochemical approach. *Polish Mineralogical Society Special Publications*, **24**, 69–72.

Bagiński, B. and Krzemińska, E. 2005. Various kinds of charnockitic rocks from NE Poland. *Polish Mineralogical Society Special Publications*, **26**, 13–17.

Bagiński, B. 2006. Different ages recorded by zircon and monazite in charnockitic rocks from the Łanowicze borehole (NE Poland). *Mineralogia Polonica Special Papers*, **29**, 79.

Bagiński, B., Kozłowski, A. and Krzemińska, E. 2006. Fluid inclusion studies – the only key to estimate the crystallization conditions of charnockitic rocks from selected boreholes from NE Poland? *Mineralogia Polonica Special Papers*, **29**, 83–86.

Bibikova, E.V, Bogdanova, S.V., Gorbatschev, R., Claesson, S. and Kirnozova, T.I. 1995. Isotopic Age, nature and structure of Precambrian crust of Belarus. *Stratigraphy and Geological correlation*, **3/6**, 591–601.

Bingen, B., Austrheim, H. and Whitehouse, M. 2001. Ilmenite as a source for zirconium during high-grade metamorphism? Textural evidence from the Caledonides of Western Norway and implication for zircon geochronology. *Journal of Petrology*, **42**, 355–375.

Black, L.P, Kamo, S.L, Allen, C.M, Davis, D.W., Aleinikoff, J.N.,Valley, J.W., Mundil, R., Campbell, I.H., Korsch, R.J., Williams, I.S. and Foudoulis, C. 2004. Improved $^{206}Pb$-$^{238}U$ microprobe geochronology by the monitoring of a trace-element-related matrix effect: SHRIMP, ID-TIMS, ELA-ICP-MS and oxygen isotope documentation for a series of zircon standards. *Chemical Geology*, **205**, 115–140.

Bogdanova, S.V., Gintov, O.B., Kurlovich, D.M., Lubnina, N.V., Nilsson, K.M., Orlyuk, M.I., Pashkevich, I.K., Shumlyanskyy, L.V. and Starostenko, V.I. 2013. Late Palaeoproterozoic mafic dyking in the Ukrainian Shield of Volgo-Sarmatia caused by rotation during the assembly of supercontinent Columbia (Nuna). *Lithos*, **174**, 196–216.

Bogdanova, S., Gorbatchev, R., Grad, M., Janik, T., Guterch, A., Kozlowskaya, E., Motuza, G., Skridlaite, G., Starostenko, I., Taran L., and Eurobridge and Polonaise working Group 2006. EUROBRIDGE: new insight into the geodynamic evolution of East European craton. In: Gee, D.G. and Stephenson, R.A. (Eds), European Lithosphere Dynamics. *Memoirs of the Geological Society of London*, **32**, 599–625.

Bogdanova, S., Gorbatschev, R., Skridlaite, G., Soesoo, A., Taran, L. and Kurlovich, D. 2015. Trans-Baltic Palaeoproterozoic correlations towards the reconstruction of supercontinent Columbia/Nuna. *Precambrian Research*, **259**, 5–33.

Brown, G.C., Thorpe, R.S. and Webb, P.C. 1984. The geochemical characteristics of granitoids in contrasting arc and comments on magma sources. *Journal of the Geological Society London*, **141**, 413–426.

Cherniak, D.J. and Watson, E.B. 2000. Pb diffusion in zircon. Chemical *Geology*, **134**, 289–301.

Claesson, S., Bogdanova, S.V., Bibikova, E.V. and Gorbatschev, R. 2001. Isotopic evidence for Palaeoproterozoic accretion in the basement of the East European Craton. *Tectonophysics*, **339**, 1–18.

Clemens, J.D. 1992. Partial melting and granulite genesis: a partisan overview. *Precambrian Research*, **55**, 297–301.

Dörr, W., Belka, Z., Marheine, D., Schastok, J., Valverde-Vaquero, P., and Wiszniewska, J. 2002. U-Pb and Ar-Ar geochronology of anorogenic granite magmatism of the Mazury Complex, NE Poland. *Precambrian Research*, **119**, 101–120.

De la Roche, H., Leterrier, J., Grandclaude, P. and Marchal, M. 1980. A classification of volcanic and plutonic rocks using R1, R2-diagrams and major element analysis – its relationships with current nomenclature. *Chemical Geology*, **29**,183–210.

Duchesne, J.-C. and Wilmart, E. 1997. Igneous charnockites and related rocks from the Bjerkreim-Sokndal layered intrusion (southwest Norway): a jotunite (hypersthene monzodiorite)-derived A-type granitoid suite. *Journal of Petrology*, **38**, 337–369.

Duchesne, J.-C., Martin, H., Bagiński, B., Vander Auwera, J. and Wiszniewska, J. 2010. The origin of the ferroan-potasic granitoids: the case of the hornblende-biotite granite suite

of the mesoproterozoic Mazury Complex, NE Poland. *The Canadian Mineralogist*, **48**, 947–968.

Ferry, J.M. and Spear, F.S. 1978. Experimental calibration of the partitioning of Fe and Mg between biotite and garnet. *Contribution to Mineralogy and Petrology*, **66**, 113–117.

Frost, R.B. and Frost, C.D. 2008. On charnockites. *Gondwana Research*, **13**, 30–44.

Frost, R.B., Frost, C.D., Hulsebosch, T.P. and Swapp, S.M. 2000. Origin of the charnockites of the Louis lake Batholith, wind River Range, Wyoming. *Journal of Petrology*, **41**, 1759–1776.

Gehrels, G. 2014. Detrital zircon U-Pb geochronology applied to tectonics. *Annual Review of Earth and Planetary Sciences*, **42**, 127–149.

Grantham, G.H., Mendonidis, P., Thomas, R.J. and Satish-Kumar, M. 2012. Multiple origins of charnockite in the Mesoproterozoic Natal belt, Kwazulu-Natal, South Africa. *Geoscience Frontiers*, **3**, 755–771.

Hansen, E.C., Janardhan, A.S., Newton, R.C., Prame, W.K.B.N. and Ravindra Kumar, G.R. 1987. Arrested charnockite formation in southern India and Sri Lanka. *Contributions to Mineralogy and Petrology*, **96**, 225–244.

Hansen, E.C., Newton, R.C., Janardhan, A.S. and Lindenberg, S. 1995. Differentiation of Late Archean crust in the eastern Dharwar Craton, Krishnagiri-Salem Area, South India. *Journal of Geology*, **103**, 629–651.

Harley, S.L., Kelly, N.M. and Möller, A. 2007. Zircon behaviour and the thermal histories of mountain chains. *Elements*, **3**, 25–30.

Henry, D.J., Guidotti, C.V, and Thomson, J.A. 2005. The Ti-saturation surface for low-to-medium pressure metapelitic biotites: Implications for geothermometry and Ti-substitution mechanisms. *Americam Mineralogist*, **90**, 316–328.

Hoskin, P.W.O. and Black, L.P. 2000. Metamorphic zircon formation by solid-state recrystallization of protolith igneous zircon. *Journal of Metamorphic Geology*, **18**, 423–439.

Janardhan, A.S., Newton, R.C., and Hansen, E.C. 1982. The transformation of amphibolites facies gneiss to charnockite in southern Karnataka and northern Tamil Nadu, India: *Contributions to Mineralogy and Petrology*, **79**, 130–149.

Janutyte, I., Majdanski, M., Voss, P.H., Kozlovskaya, E. and PASSEQ Working Group. 2015. Upper mantle structure around the Trans-European Suture Zone obtained by teleseismic tomography. *Solid Earth*, **6**, 73–91.

Jenner, G.A., Dunnling, G.R., Malpas, J.J., Brown, M. and Brace, T. 1991. Bay of Islands and Little Port complexes revisited: age, geochemical and isotopic evidence confirm suprasubduction-zone origin. *Canadian Journal of Earth Sciences*, **28**, 1635–1652.

Kilpatrick, J.A. and Ellis, D.J. 1992. C-type magmas: igneous charnockites and their extrusive equivalents. *Transactions Royal Society Edinburgh: Earth Sciences*, **83**, 155–164.

Kleinfeld, B. and Olesch, M. 2000. Imprint of different fluid generations on granulitic gneisses from central Dronning Maud Land, Antarctica. *Journal Geochemistry. Exploration*, **69-70**, 349–352.

Kohn, M.J, Corrie, S.L. and Markley, C. 2015. The fall and rise of metamorphic zircon. *American Mineralogist*, **100**, 897–908.

Kohn, M.J. and Kelly, N.M. 2018. Petrology and Geochronology of Metamorphic Zircon. In: Moser, D.E., Corfu, F., Darling, J.R., Reddy, S.M. and Tait, K. (Eds), Microstructural Geochronology: Planetary Records Down to Atom Scale. *Geophysical Monograph Series*, **232**, 35–61. American Geophysical Union; Hoboken and John Wiley & Sons, Inc.; Washington, D.C.

Kovaleva, E., Klötzli, U., Habler, G. and Libowitzky, E. 2014. Finite lattice distortion patterns in plastically deformed zircon grains. *Solid Earth*, **5**, 1099–1122.

Kröner, A., Wan Y., Liu X. and Dunyi, L. 2014. Dating of zircon from high-grade rocks: Which is the most reliable method? *Geoscience Frontiers*, **5**, 515–523.

Krzemińska, E. and Wiszniewska, J. 2017. Magma generation processes within Mazury AMCG suite (EEC), evidence from inherited zircons. Goldschmidt Abstracts, 2017, 2130.

Krzemińska, E., Krzemiński, L., Petecki, Z., Wiszniewska, J., Salwa, S., Żaba, J., Gaidzik, K., Williams, I.S., Rosowiecka, O., Taran, L., Johansson, Å., Pécskay, Z., Demaiffe, D., Grabowski, J. and Zieliński, G. 2017. Geological map of crystalline basement in the Polish part of East European Platform, 1:1 000 000. Państwowy Instytut Geologiczny, Warszawa. [In Polish with English summary]

Krzemińska, E., Williams, I. and Wiszniewska, J. 2005. A Late Palaeoproterozoic (1.80 Ga) subduction-related mafic igneous suite from Łomża, NE Poland. *Terra Nova*, **17**,442–449.

Kunz, B.E,·Regis,·D. and Engi, D.M. 2018. Zircon ages in granulite facies rocks: decoupling from geochemistry above 850°C? *Contributions to Mineralogy and Petrology*, **173**, 26.

Lahtinen, R., Korja, A., and Nironen, M. 2005. Palaeoproterozoic tectonic evolution. In: Lehtinen, M., Nurmi, P.A. and Rämö, O.T. (Eds), Precambrian Geology of Finland – Key to the Evolution of the Fennoscandian Shield, 481–532. Elsevier; Amsterdam.

Ludwig, K.R. 2004. Isoplot/Ex: A Geochronological Toolkit for Microsoft Excel. *Berkeley Geochronology Center*, *Special Publication*, **1a** (rev. 3).

Ludwig, K. 2009. SQUID 2: A User's Manual, rev. 12 Apr, 2009. *Berkeley Geochronology Center*, *Special Publication*, **5**, 1–110.

Maniar, P.D. and Piccoli, P.M. 1989. Tectonic discrimination of granitoids. *Geological Society of America Bulletin*, **101**, 635–643.

Mansfeld, J. 2001. Age and εNd constraints on the Palaeoproterozoic tectonic evolution in the Baltic-Sea region. *Tectonophysics*, **339**, 135–151.

Mezger, K. and Krogstad, E.J. 1997. Interpretation of discordant U-Pb zircon ages: An evaluation. *Journal of Metamorphic Geology*, **15**, 127–140.

Morgan, J.W., Stein, H.J., Hannah, J.L., Markey, R.J. and Wiszniewska, J. 2000. Re-Os study of Fe-Ti-V oxide and Fe-Cu-Ni sulfide deposits, Suwałki Anortosite Massif, Northeast Poland. *Mineralium Deposita*, **35**, 391–401.

Morimoto, N. and Subcommittee on Pyroxenes. 1989. Nomenclature of pyroxenes. *The Canadian Mineralogist*, **27**, 143–156.

Motuza, G. 2005. Structure and formation of the crystalline crust in Lithuania. *Mineralogical Society of Poland*, *Special Papers*, **26**, 69–79.

Motuza, G. and Motuza, V. 2011. Charnockitic rocks in the crystalline basement of Western Lithuania: implications on their origin and correlation with the Askersund suite in SE Sweden. *Geological Quarterly*, **55**, 63–70.

Motuza, G., Motuza, V., Salnikova, E.B. and Kotov, A.B. 2008. Extensive charnockitic-granitic magmatism in the crystalline crust of West Lithuania. *Geologia*, **61**, 1–16.

Müller, D. and Groves, D.I. 1997. Potassic igneous rocks and associated gold-copper mineralization. *Lecture Notes in Earth Sciences*, **238**, 1–84.

Pearce, J.A., Harris, N.B.W. and Tindle, A.G. 1984. Trace element discrimination diagrams for the Tectonic Interpretation of Granitic Rocks. *Journal of Petrology*, **25**, 956–983.

Perchuk, L.L. and Gerya, T.V. 1993. Fluid control of charnockitization. *Chemical Geology*, **108**, 175–186.

Rajesh, H.M and Santosh, M. 2012. Charnockites and charnockites. *Geoscience Frontiers*, **3**, 737–744.

Reimink, J.R., Davies, J.H., Waldron, J.W. and Rojas, X. 2016. Dealing with discordance: a novel approach for analysing U-Pb detrital zircon datasets. *Journal of the Geological Society of London*, **173**, 577–585.

Rimsa, A., Bogdanova, S.V., Skridlaite, G. and Bibikova, E. 2001. The Randamonys TTG-intrusion in southern Lithuania: evidence of a 1.84 Ga island arc. *Journal of Conference Abstracts*, **6**, 368–359.

Rubatto, D. 2002. Zircon trace element geochemistry: Partitioning with garnet and the link between U-Pb ages and metamorphism. *Chemical Geology*, **184**, 123–138.

Rubatto, D. 2017. Zircon: The metamorphic mineral. *Reviews in Mineralogy and Geochemistry*, **83**, 261–295.

Schoene, B. 2014. U-Th-Pb geochronology. In: Treatise on Geochemistry 2nd Edition, pp. 341–378. Elsevier; Amsterdam.

Shumlyanskyy, L., Ernst, R.E., Söderlund, U., Billström, K., Mitrokhin, O. and Tsymbal, S. 2016. New U-Pb ages for mafic dykes in the Northwestern region of the Ukrainian shield: coeval tholeiitic and jotunitic magmatism. *GFF*, **138**, 79–85.

Skridlaite, G. and Motuza, G. 2001. Precambrian domains in Lithuania: evidence of terrane tectonics. *Tectonophysics*, **339**, 113–133.

Skridlaite, G., Wiszniewska, J. and Duchesne, J.-C. 2003. Ferropotassic A-type granites and related rocks in NE Poland and S Lithuania: west of the East European Craton. *Precambrian Research*, **124**, 305–326.

Skridlaite, G., Bagiński, B. and Whitehouse, M. 2008. Significance of ~1.5 Ga zircon and monazite ages from charnockites in Southern Lithuania and NE Poland. *Gondwana Research*, **14**, 663–674.

Skridlaite, G., Bogdanova, S.V., Taran, L., Bagiński, B., Krzemińska, E., Wiszniewska, J. and Whitehouse, M. 2009. Over 400 m.y. metamorphic history of the Fennoscandian lithospheric segment in the Proterozoic (the East European Craton). *Geophysical Research Abstracts*, 11, EGU2009-9095-1. EGU General Assembly.

Skridlaite, G., Bogdanova, S., Taran, L. and Bagiński, B. 2014. Recurrent high grade metamorphism recording a 300 Ma long Proterozoic crustal evolution in the western part of the East European Craton. *Gondwana Research*, **25**, 649–667.

Skridlaite, G., Whitehouse, M., Bogdanova, S. and Taran, L. 2011. The 1.86–1.84 Ga magmatism in the Western East European Craton (Lithuania): implications for a convergent continental margin. *International Goldschmidt Conference Abstracts*, **75** (3), 1890.

Siliauskas, L., Skridlaite, G., Bagiński, B., Whitehouse, M. and Prusinskiene, S. 2018a. What the ca. 1.83 Ga gedrite-cordierite schists in the crystalline basement of Lithuania tell us about the late Palaeoproterozoic accretion of the East European Craton. *GFF*, **140**, 332–344.

Siliauskas, L., Skridlaite, G., Whitehouse, M., and Soesoo, A. 2018b. A ca. 1.89 Ga magmatic complex in eastern Lithuania: a link connecting with the domains in Estonia and Bergslagen terrane in Sweden. Abstracts in 33rd Nordic Geological Winter Meeting, 10th–12th January 2016, Copenhagen, Denmark, p. 59. Dansk Geologisk Forening, Geological Society of Denmark.

Spencer, Ch.J., Kirkland, K.L. and Taylor, R.J.M. 2016. Strategies towards statistically robust interpretations of in situ U-Pb zircon geochronology. *Geoscience Frontiers*, **7**, 581–589.

Stern, R.J. and Dawoud, A.S. 1991. Late Precambrian (740 Ma) charnockite, enderbite, and granite from Jebel Moya, Sudan: a link between the Mozambique Belt and the Arabian-Nubian Shield? *Journal of Geology*, **99**, 648–659.

Stern, R.A., Bodorkos, S., Kamo, S.L., Hickman, A.H., and Corfu, F. 2009. Measurement of SIMS instrumental mass fractionation of Pb-isotopes during zircon dating. *Geostandards and Geoanalytical Research*, **33**, 145–168.

Tera, F. and Wasserburg, G. 1972. U-Th-Pb systematics in lunar highland samples from the Luna 20 and Apollo 16 missions. *Earth and Planetary Science Letters*, **17**, 36–51.

Touret, J.L.R. and Huizenga, J.M 2012. Charnockite microstructures: From Magmatic to metamorphic. *Geoscience Frontiers*, **3** (6), 745–753.

Van der Kerkhof, A.M. and Grantham, G.H. 1999. Metamorphic charnockite in contact aureoles around intrusive enderbite from Natal. *Contributions to Mineralogy and Petrology*, **137**, 115–132.

Wan, Y.S., Liu, D.Y., Dong Ch., Liu, S., Wang, S. and Yang, E. 2011. U-Th-Pb behavior of zircons under high-grade metamorphic conditions: A case study of zircondating of metadiorite near Qixia, eastern Shandong. *Geoscience Frontiers*, **2**, 137–146.

Whitney, D.L. and Evans, B.W. 2010. Abbreviations for names of rock-forming minerals *American Mineralogist*, **95**, 185–187.

Williams, I.S. 1998. U-Th-Pb Geochronology by Ion Microprobe. In: McKibben, M.A., Shanks III, W.C. and Ridley, W.I. (Eds), Application of Microanalytical Techniques to Understanding Mineralizing Processes. *Reviews in Economic Geology*, **7**, 1–35.

Wiszniewska, J. 2002. Age and the genesis of Fe-Ti-V ores and related rocks in the Suwałki Anorthozite Massif (northeastern Poland). *Biuletyn Państwowego Instytutu Geologicznego*, **401**, 1–96. [In Polish with English abstract]

Wiszniewska, J., Krzemińska, E., Williams, I.S. and Krzemiński, L. 2016. AMCG suite in NE Poland; subsequent datings of A-type granitoids on SHRIMP. 8th SHRIMP Workshop, 6–10 September 2016, Granada, Abstracts Volume, 87–89, University of Granada; Spain.

Wiszniewska, J. and Krzemińska, E. 2017. Peraluminous vein granites from the Suwałki Anorthosite Massif and their tectonic significance – evidence from zircon age study by SHRIMP IIe/MC. *Mineralogia, Special Papers*, **47**, 40.

Wybraniec, S. 1999. Transformation and visualization of potential field data. *Special Papers of the Polish Geological Institute*, **1**, 1–88.

*Manuscript submitted: 21st January 2019*
*Revised version accepted: 11th June 2019*

**Suppl. Table 1. Whole-rock analyses of charnockite samples selected from the Łanowicze PIG-1 borehole**

| | depth (m) | | granitogneisse unit | | | | | | | granulite unit | | | |
|---|---|---|---|---|---|---|---|---|---|---|---|---|---|
| wt % | 1111.5 | 1162 | 1177 | 1188- | 1293 | 1354.8 | 1366.5 | 1381.6 | 1402 | 1412 | 1472 | 1473 | 1485 |
| $SiO_2$ | 57.86 | 62.04 | 60.98 | 62.08 | 65.16 | 68.12 | 69.8 | 67.81 | 68.07 | 68.32 | 68.03 | 64.9 | 68.82 |
| $TiO_2$ | 1.56 | 1.04 | 1.09 | 1.03 | 0.76 | 0.38 | 0.6 | 0.63 | 0.69 | 0.61 | 0.62 | 0.84 | 0.76 |
| $Al_2O_3$ | 14.95 | 15.02 | 15.87 | 15.95 | 15.38 | 14.84 | 13.71 | 14.55 | 14.4 | 14.16 | 14.6 | 14.9 | 13.66 |
| $Fe_2O_3t$ | 12.51 | 8.13 | 7.82 | 7.78 | 5.48 | 2.64 | 2.16 | 4.21 | 4.72 | 4.27 | 4.37 | 5.99 | 4.7 |
| MnO | 0.18 | 0.13 | 0.11 | 0.14 | 0.9 | 0.04 | 0.03 | 0.06 | 0.06 | 0.05 | 0.06 | 0.08 | 0.05 |
| MgO | 3.09 | 2.21 | 2 | 2.11 | 1.46 | 0.8 | 0.9 | 1.08 | 1.27 | 1.25 | 1.09 | 1.57 | 0.93 |
| CaO | 4.42 | 3.77 | 4.22 | 3.93 | 3.52 | 1.61 | 1.24 | 2.84 | 2.8 | 2.3 | 3 | 3.25 | 2.38 |
| $Na_2O$ | 2.71 | 2.71 | 3.08 | 2.93 | 2.83 | 2.61 | 2.09 | 2.74 | 2.76 | 2.54 | 2.66 | 2.88 | 2.42 |
| $K_2O$ | 1.71 | 3.07 | 3.25 | 2.72 | 3.82 | 6.56 | 7.47 | 4.48 | 3.86 | 4.61 | 3.87 | 4.15 | 4.56 |
| $P_2O_5$ | 0.21 | 0.15 | 0.23 | 0.26 | 0.13 | 0.21 | 0.24 | 0.18 | 0.13 | 0.16 | 0.11 | 0.21 | 0.22 |
| ppm | | | | | | | | | | | | | |
| U | 2.1 | 1.3 | 1.4 | 1.7 | 1.6 | 4 | 0.9 | 2.1 | 1.8 | 1.6 | 1.4 | 2 | 1.8 |
| Th | 45.8 | 34.1 | 28.4 | 22.5 | 17.9 | 131.9 | 174.4 | 21.6 | 21.4 | 16.8 | 23.8 | 24.2 | 21.3 |
| Th/U | 21.8 | 26.2 | 20.3 | 13.2 | 11.2 | 33.0 | 193.8 | 10.3 | 11.9 | 10.5 | 17.0 | 12.1 | 11.8 |
| Zr | 514.3 | 349.7 | 352.5 | 334.9 | 203.3 | 306.4 | 473.4 | 237.4 | 232.8 | 198.9 | 214.8 | 321.3 | 325.8 |
| Hf | 15.2 | 11.3 | 10.4 | 10.4 | 6 | 10 | 13 | 7 | 7 | 6 | 7 | 9 | 10 |
| Zr/Hf | 34 | 31 | 34 | 32 | 33 | 32 | 36 | 34 | 34 | 32 | 30 | 36 | 34 |
| Nb | 17.2 | 13 | 17.7 | 15.2 | 11.3 | 19.1 | 17.3 | 11.4 | 11.4 | 11.1 | 12 | 15.2 | 14 |
| Ta | 0.6 | 0.6 | 0.9 | 0.7 | 0.6 | 0.9 | 0.4 | 0.5 | 0.5 | 0.50 | 0.60 | 0.7 | 0.6 |
| Nb/Ta | 29 | 22 | 20 | 22 | 19 | 21 | 43 | 23 | 23 | 22 | 20 | 22 | 23 |
| Rb | 85.7 | 117.1 | 11.2 | 116.7 | 140.3 | 323.1 | 276.8 | 169.5 | 155.8 | 172.9 | 153.7 | 154.8 | 178.3 |
| Cs | 1.6 | 1.6 | 1.1 | 1.2 | 1.4 | 2.2 | 0.6 | 1.6 | 1.3 | 1.30 | 1.00 | 1.3 | 1.3 |
| Sr | 179.5 | 213.6 | 291.4 | 171.3 | 198.8 | 192 | 206.5 | 157.2 | 165.2 | 147 | 210.3 | 180.7 | 148.6 |
| Ba | 451.4 | 1087 | 1128.9 | 671 | 1057.3 | 779.2 | 1167 | 880.9 | 766.5 | 844.8 | 1338.4 | 866 | 926.1 |
| K/Rb | 1212 | 576 | 5797 | 553 | 324 | 68 | 65 | 206 | 252 | 205 | 236 | 321 | 219 |
| K/Ba | 230 | 62 | 58 | 96 | 43 | 28 | 15 | 40 | 51 | 42 | 27 | 57 | 42 |
| Rb/Sr | 0.48 | 0.55 | 0.04 | 0.68 | 0.71 | 1.68 | 1.34 | 1.08 | 0.94 | 1.18 | 0.73 | 0.86 | 1.20 |
| Rb/Cs | 54 | 73 | 10 | 97 | 100 | 147 | 461 | 106 | 120 | 133 | 154 | 119 | 137 |
| Ni | 121.9 | 23.3 | 104.3 | 22.6 | 101 | 5.4 | 32.7 | 29.6 | 40.1 | 36.3 | 25 | 47.2 | 27.8 |
| V | 161 | 119 | 92 | 98 | 68 | 28 | 33 | 51 | 60 | 53 | 51 | 71 | 45 |
| Zn | 94 | 68 | 62 | 95 | 46 | 54 | 27 | 42 | 44 | 39 | 37 | 64 | 45 |
| Co | 28.1 | 22.4 | 21.4 | 20.1 | 14.4 | 5.2 | 7.1 | 11.1 | 11.4 | 9 | 11.3 | 13.9 | 9.4 |
| Cu | 56.1 | 23.7 | 20.8 | 29.9 | 32.7 | 71.3 | 57.9 | 15.7 | 14.2 | 17.3 | 12.5 | 25.3 | 36.7 |
| Ga | 29.6 | 24.5 | 25.2 | 25.9 | 19.6 | 23.4 | 14.3 | 19.7 | 17.7 | 18.3 | 20.2 | 22.2 | 18.6 |
| Pb | 8.1 | 6.4 | 5.9 | 5.4 | 5.6 | 17.3 | 19.9 | 5.2 | 4.9 | 5.3 | 5.9 | 4.7 | 5.9 |
| Y | 49.6 | 33.6 | 46.3 | 48.7 | 25.4 | 25.2 | 35.9 | 33.1 | 27.6 | 34.1 | 21.7 | 46.4 | 38.7 |
| La | 104.9 | 84.5 | 74.1 | 70 | 52.9 | 160.1 | 183.7 | 56.1 | 53.8 | 48.1 | 61.5 | 58.5 | 67.8 |
| Ce | 233.3 | 192.1 | 177.3 | 142.3 | 115.2 | 386.5 | 434.1 | 116.2 | 111.4 | 94.9 | 121.7 | 136.6 | 135.9 |
| Pr | 25.69 | 20.16 | 19.04 | 15.15 | 12.4 | 44.05 | 51.07 | 13.46 | 12.98 | 11.18 | 13.71 | 14.82 | 15.49 |
| Nd | 102.3 | 78.1 | 74.7 | 64.2 | 44.1 | 160.8 | 192.4 | 49.1 | 50.1 | 42 | 48.4 | 62.2 | 61.6 |
| Sm | 16.3 | 12.2 | 12.3 | 11.9 | 7.9 | 24.9 | 33.8 | 10.6 | 9.7 | 8.8 | 9.5 | 10.4 | 12 |
| Eu | 1.96 | 2.3 | 2.54 | 1.69 | 2.19 | 2.05 | 2.35 | 1.68 | 1.67 | 1.57 | 2.23 | 1.62 | 1.88 |
| Gd | 13.12 | 9.66 | 9.48 | 10.42 | 5.93 | 10.36 | 17.98 | 7.99 | 7.38 | 6.87 | 6.48 | 8.74 | 8.71 |
| Tb | 2.06 | 1.36 | 1.53 | 1.65 | 0.89 | 1.15 | 2.14 | 1.14 | 1.03 | 0.96 | 0.87 | 1.67 | 1.29 |
| Dy | 9.11 | 6.24 | 7.26 | 9.25 | 4.73 | 5.07 | 8.89 | 6.49 | 5.6 | 6.4 | 4.8 | 7.66 | 7.38 |
| Ho | 1.7 | 1.09 | 1.35 | 1.57 | 0.87 | 0.77 | 1.23 | 1.18 | 0.88 | 1.23 | 0.72 | 1.46 | 1.28 |
| Er | 3.98 | 2.86 | 3.64 | 4.09 | 2.15 | 1.86 | 2.4 | 2.55 | 1.98 | 3.04 | 1.6 | 3.73 | 3.33 |
| Tm | 0.57 | 0.4 | 0.49 | 0.55 | 0.3 | 0.3 | 0.29 | 0.35 | 0.29 | 0.47 | 0.24 | 0.49 | 0.45 |
| Yb | 3.71 | 2.62 | 2.92 | 3.57 | 1.98 | 1.8 | 1.77 | 2.2 | 1.73 | 2.96 | 1.12 | 2.25 | 2.72 |
| Lu | 0.54 | 0.43 | 0.45 | 0.48 | 0.33 | 0.25 | 0.25 | 0.3 | 0.27 | 0.5 | 0.23 | 0.4 | 0.41 |

**Suppl. Table 2. U-Pb SHRIMP analyses of zircon grains from charnockite rocks from the Łanowicze PIG-1 borehole**

**Łanowicze 1162**

| Spot | $^{204}Pb/^{206}Pb$ | ±% | $^{207}Pb/^{206}Pb$ | ±% | $^{208}Pb/^{206}Pb$ | ±% | $^{206}Pb/^{238}U$ | ±% | %$^{206}Pbc$ | $^{232}Th/^{238}U$ | ±% | (1) $^{206}Pb/^{238}U$ Age | | (2) 206Pb/238U Age | | (3) 206Pb/238U Age | | (1) 207Pb/206Pb Age | | (1)208Pb/232Th Age | | % Discordant | 7corr $^{208}Pb^*/^{232}Th$ | ±% | (1) $^{238}U/^{206}Pb^*$ | ±% | (1) $^{207}Pb^*/^{206}Pb^*$ | ±% | (1) $^{207}Pb^*/^{235}U$ | ±% | (1) $^{206}Pb^*/^{238}U$ | ±% | err corr |
|---|---|---|---|---|---|---|---|---|---|---|---|---|---|---|---|---|---|---|---|---|---|---|---|---|---|---|---|---|---|---|---|---|
| A.1.1 | 3.7E-5 | 58 | 0.1127 | 1.91 | 0.041 | 1.8 | 1.075 | 0.7 | 2.0E-2 | 0.11 | 1.4 | 1783 | ±40 | 1775 | ±46 | 1776 | ±41 | 1836 | ±35 | 2272 | ±87 | +3 | 0.0873 | 36.8 | 3.139 | 2.6 | 0.1122 | 1.94 | 4.93 | 3.2 | 0.3186 | 2.6 | 0.80 |
| A.3.1 | -2.4E-5 | 71 | 0.1135 | 0.67 | 0.169 | 0.9 | 1.176 | 2.3 | 1.0E-2 | 0.46 | 1.4 | 1831 | ±42 | 1826 | ±49 | 1800 | ±45 | 1862 | ±13 | 2334 | ±70 | +2 | 0.1179 | 6.4 | 3.044 | 2.6 | 0.1138 | 0.70 | 5.16 | 2.7 | 0.3285 | 2.6 | 0.97 |
| A.2.1 | 2.6E-5 | 50 | 0.1112 | 0.52 | 0.025 | 1.7 | 1.124 | 0.9 | 1.4E-4 | 0.07 | 1.2 | 1878 | ±38 | 1888 | ±44 | 1874 | ±38 | 1814 | ±10 | 2266 | ±81 | -4 | 0.1857 | 23.2 | 2.957 | 2.3 | 0.1109 | 0.54 | 5.17 | 2.4 | 0.3381 | 2.3 | 0.97 |
| A.5.1 | -2.6E-5 | 59 | 0.0975 | 0.62 | 0.033 | 6.0 | 0.760 | 0.45 | – | 0.08 | 0.92 | 1565 | ±30 | 1564 | ±33 | 1557 | ±31 | 1583 | ±12 | 2355 | ±149 | +1 | 0.113 | 18 | 3.638 | 2.2 | 0.09782 | 0.65 | 3.707 | 2.3 | 0.2749 | 2.2 | 0.96 |
| A.11.1 | -8.6E-6 | 73 | 0.1096 | 0.41 | 0.020 | 1.8 | 1.039 | 0.29 | – | 0.06 | 0.65 | 1772 | ±32 | 1769 | ±37 | 1770 | ±33 | 1795 | ±8 | 2005 | ±58 | +1 | 0.082 | 40 | 3.160 | 2.1 | 0.10973 | 0.41 | 4.787 | 2.1 | 0.3164 | 2.1 | 0.98 |
| A.18.1 | -4.1E-5 | 45 | 0.1127 | 0.55 | 0.199 | 0.7 | 1.108 | 0.78 | – | 0.56 | 0.86 | 1794 | ±36 | 1785 | ±41 | 1761 | ±39 | 1852 | ±11 | 2211 | ±54 | +4 | 0.109 | 5 | 3.117 | 2.3 | 0.11326 | 0.59 | 5.010 | 2.4 | 0.3208 | 2.3 | 0.97 |
| A.15.1 | -1.1E-4 | 35 | 0.1101 | 0.70 | 0.172 | 1.0 | 1.134 | 0.99 | – | 0.47 | 1.09 | 1805 | ±30 | 1802 | ±35 | 1772 | ±33 | 1826 | ±15 | 2324 | ±56 | +1 | 0.119 | 5 | 3.094 | 1.9 | 0.11160 | 0.83 | 4.974 | 2.1 | 0.3232 | 1.9 | 0.92 |
| A.16.1 | -1.7E-5 | 90 | 0.1123 | 0.71 | 0.182 | 1.0 | 1.100 | 1.01 | – | 0.53 | 1.09 | 1807 | ±39 | 1802 | ±45 | 1782 | ±42 | 1840 | ±13 | 2152 | ±59 | +2 | 0.108 | 6 | 3.091 | 2.5 | 0.11249 | 0.73 | 5.018 | 2.6 | 0.3235 | 2.5 | 0.96 |
| A.7.1 | -3.4E-5 | 50 | 0.1118 | 0.56 | 0.098 | 1.0 | 1.034 | 0.46 | – | 0.27 | 0.86 | 1815 | ±36 | 1812 | ±42 | 1798 | ±37 | 1837 | ±11 | 2289 | ±59 | +1 | 0.115 | 8 | 3.075 | 2.3 | 0.11231 | 0.59 | 5.036 | 2.4 | 0.3252 | 2.3 | 0.97 |
| A.8.1 | -1.3E-4 | 27 | 0.1106 | 0.57 | 0.074 | 1.2 | 0.926 | 0.78 | – | 0.21 | 0.84 | 1825 | ±36 | 1823 | ±41 | 1811 | ±37 | 1837 | ±13 | 2324 | ±69 | +1 | 0.118 | 10 | 3.056 | 2.2 | 0.11232 | 0.69 | 5.068 | 2.3 | 0.3272 | 2.2 | 0.96 |
| A.17.1 | 1.8E-5 | 77 | 0.1134 | 0.61 | 0.091 | 3.6 | 1.023 | 0.43 | 0.03 | 0.26 | 0.92 | 1828 | ±32 | 1825 | ±36 | 1816 | ±33 | 1851 | ±11 | 2166 | ±87 | +1 | 0.107 | 9 | 3.050 | 2.0 | 0.11315 | 0.63 | 5.115 | 2.1 | 0.3279 | 2.0 | 0.95 |
| A.13.1 | -4.2E-5 | 41 | 0.1119 | 0.50 | 0.032 | 1.5 | 1.024 | 0.41 | – | 0.09 | 0.81 | 1846 | ±35 | 1847 | ±41 | 1839 | ±36 | 1839 | ±10 | 2383 | ±77 | -0 | 0.130 | 22 | 3.017 | 2.2 | 0.11245 | 0.54 | 5.140 | 2.3 | 0.3315 | 2.2 | 0.97 |
| A.14.1 | -2.7E-5 | 59 | 0.1115 | 0.58 | 0.067 | 1.2 | 1.137 | 0.85 | – | 0.19 | 0.92 | 1852 | ±37 | 1856 | ±43 | 1841 | ±38 | 1830 | ±11 | 2286 | ±63 | -1 | 0.128 | 12 | 3.004 | 2.3 | 0.11186 | 0.61 | 5.134 | 2.4 | 0.3328 | 2.3 | 0.97 |
| A.12.1 | -3.2E-5 | 45 | 0.1111 | 0.90 | 0.031 | 1.5 | 1.045 | 0.34 | – | 0.09 | 0.47 | 1857 | ±35 | 1862 | ±41 | 1851 | ±35 | 1824 | ±17 | 2372 | ±72 | -2 | 0.152 | 21 | 2.995 | 2.2 | 0.11149 | 0.91 | 5.132 | 2.4 | 0.3339 | 2.2 | 0.92 |
| A.4.1 | -4.2E-5 | 45 | 0.1108 | 0.55 | 0.129 | 1.9 | 1.065 | 0.79 | – | 0.34 | 0.88 | 1872 | ±37 | 1880 | ±43 | 1846 | ±39 | 1823 | ±11 | 2443 | ±72 | -3 | 0.139 | 7 | 2.968 | 2.3 | 0.11141 | 0.59 | 5.176 | 2.3 | 0.3370 | 2.3 | 0.97 |
| A.6.1 | -1.5E-5 | 71 | 0.1114 | 0.51 | 0.024 | 1.8 | 1.060 | 0.74 | – | 0.07 | 0.80 | 1876 | ±49 | 1884 | ±58 | 1872 | ±50 | 1826 | ±9 | 2357 | ±89 | -3 | 0.177 | 32 | 2.961 | 3.0 | 0.11162 | 0.52 | 5.198 | 3.1 | 0.3377 | 3.0 | 0.99 |
| A.10.1 | -1.0E-4 | 45 | 0.1131 | 0.84 | 0.178 | 1.1 | 1.021 | 1.16 | – | 0.48 | 1.27 | 1897 | ±44 | 1902 | ±52 | 1861 | ±47 | 1872 | ±18 | 2442 | ±76 | -2 | 0.132 | 6 | 2.922 | 2.7 | 0.11449 | 0.98 | 5.402 | 2.8 | 0.3422 | 2.7 | 0.94 |
| A.9.1 | -1.1E-4 | 27 | 0.1403 | 0.48 | 0.070 | 1.1 | 1.224 | 0.79 | – | 0.17 | 0.90 | 2038 | ±39 | 1990 | ±46 | 2015 | ±40 | 2249 | ±9 | 3094 | ±89 | +11 | 0.039 | 54 | 2.690 | 2.3 | 0.14177 | 0.55 | 7.267 | 2.3 | 0.3718 | 2.3 | 0.97 |

Errors are 1-sigma; Pbc and Pb* indicate the common and radiogenic portions, respectively. Error in Standard calibration was 0.64% (not included in above errors but required when comparing data from different mounts). (1) Common Pb corrected using measured $^{204}Pb$. (2) Common Pb corrected by assuming $^{206}Pb/^{238}U$–$^{207}Pb/^{235}U$ age-concordance (3) Common Pb corrected by assuming $^{206}Pb/^{238}U$–$^{208}Pb/^{232}Th$ age-concordance

**Łanowicze 1381**

| Spot | $^{204}Pb/^{206}Pb$ | ±% | $^{207}Pb/^{206}Pb$ | ±% | $^{208}Pb/^{206}Pb$ | ±% | $^{206}Pb/^{238}U$ | ±% | % $^{206}Pbc$ | $^{232}Th/^{238}U$ | ±% | (1) $^{206}Pb/^{238}U$ | Age | (2) $^{206}Pb/^{238}U$ | Age | (3) $^{206}Pb/^{238}U$ | Age | (1) $^{207}Pb/^{206}Pb$ | Age | (1) $^{208}Pb/^{232}Th$ | Age | % Discordant | 7corr $^{208}Pb^*/^{232}Th$ | ±% | (1) $^{238}U/^{206}Pb^*$ | ±% | (1) $^{207}Pb^*/^{206}Pb^*$ | ±% | (1) $^{207}Pb^*/^{235}U$ | ±% | (1) $^{206}Pb^*/^{238}U$ | ±% | errcorr |
|---|---|---|---|---|---|---|---|---|---|---|---|---|---|---|---|---|---|---|---|---|---|---|---|---|---|---|---|---|---|---|---|---|
| B.14.1 | 3.0E-5 | 58 | 0.0947 | 0.66 | 0.028 | 5.0 | 0.942 | 1.0 | 0.03 | 0.08 | 1.3 | 1497 | ±33 | 1495 | ±36 | 1494 | ±33 | 1515 | ±13 | 1799 | ±107 | +1 | 0.0835 | 22.7 | 3.827 | 2.5 | 0.0943 | 0.71 | 3.40 | 2.6 | 0.2613 | 2.5 | 0.96 |
| B.8.1 | 6.5E-5 | 58 | 0.1123 | 0.89 | 0.189 | 1.2 | 0.728 | 1.2 | 0.41 | 0.37 | 1.5 | 1577 | ±36 | 1548 | ±39 | 1521 | ±39 | 1824 | ±18 | 2654 | ±82 | +15 | 0.1078 | 5.5 | 3.608 | 2.6 | 0.1115 | 1.01 | 4.26 | 2.8 | 0.2772 | 2.6 | 0.93 |
| B.41.1 | -1.4E-5 | 100 | 0.1064 | 0.74 | 0.206 | 0.9 | 1.140 | 1.1 | 0.26 | 0.53 | 1.5 | 1693 | ±39 | 1686 | ±43 | 1653 | ±42 | 1742 | ±14 | 2225 | ±66 | +3 | 0.1113 | 4.9 | 3.330 | 2.6 | 0.1066 | 0.76 | 4.41 | 2.7 | 0.3003 | 2.6 | 0.96 |
| B.14.2 | -1.9E-5 | 100 | 0.1102 | 1.41 | 0.141 | 1.3 | 1.232 | 2.5 | 0.15 | 0.39 | 0.7 | 1689 | ±44 | 1673 | ±49 | 1666 | ±47 | 1807 | ±26 | 2112 | ±67 | +7 | 0.0931 | 8.3 | 3.340 | 3.0 | 0.1104 | 1.43 | 4.56 | 3.3 | 0.2994 | 3.0 | 0.90 |
| B.47.1 | – | – | 0.1140 | 0.53 | 0.117 | 0.9 | 1.115 | 1.6 | 0.14 | 0.30 | 1.2 | 1715 | ±36 | 1694 | ±40 | 1693 | ±37 | 1865 | ±10 | 2238 | ±60 | +9 | 0.0883 | 8.0 | 3.282 | 2.4 | 0.1140 | 0.53 | 4.79 | 2.4 | 0.3047 | 2.4 | 0.98 |
| B.18.1 | -8.4E-5 | 50 | 0.1102 | 1.74 | 0.170 | 1.2 | 1.101 | 1.3 | 0.21 | 0.44 | 1.7 | 1732 | ±44 | 1719 | ±50 | 1697 | ±47 | 1821 | ±33 | 2300 | ±80 | +6 | 0.1086 | 7.5 | 3.245 | 2.9 | 0.1113 | 1.79 | 4.73 | 3.4 | 0.3081 | 2.9 | 0.85 |

| | | | | | | | | | | | | | | | | | | | | | | | | | | | | | | | | | |
|---|---|---|---|---|---|---|---|---|---|---|---|---|---|---|---|---|---|---|---|---|---|---|---|---|---|---|---|---|---|---|---|---|---|
| B.40.1 | – | – | 0.1103 | 0.82 | 0.057 | 1.1 | 1.152 | 0.9 | 0.07 | 0.15 | 1.2 | 1731 | ±36 | 1720 | ±40 | 1721 | ±36 | 1805 | ±15 | 2234 | ±61 | +5 | 0.0877 | 17.1 | 3.247 | 2.3 | 0.1103 | 0.82 | 4.69 | 2.5 | 0.3080 | 2.3 | 0.94 |
| B.15.1 | – | – | 0.1133 | 0.92 | 0.308 | 1.0 | 1.111 | 1.4 | 0.39 | 0.81 | 1.7 | 1800 | ±46 | 1792 | ±53 | 1739 | ±53 | 1853 | ±17 | 2321 | ±77 | +3 | 0.1175 | 4.8 | 3.104 | 2.9 | 0.1133 | 0.92 | 5.03 | 3.1 | 0.3222 | 2.9 | 0.95 |
| B.31.1 | 3.2E-5 | 58 | 0.1080 | 0.66 | 0.183 | 0.9 | 1.135 | 1.1 | 0.19 | 0.50 | 1.4 | 1772 | ±39 | 1774 | ±44 | 1743 | ±42 | 1759 | ±13 | 2186 | ±62 | -1 | 0.1158 | 5.2 | 3.161 | 2.5 | 0.1076 | 0.70 | 4.69 | 2.6 | 0.3164 | 2.5 | 0.96 |
| B.46.1 | -3.4E-5 | 38 | 0.1117 | 0.46 | 0.018 | 1.7 | 1.087 | 0.5 | 0.19 | 0.05 | 2.4 | 1750 | ±35 | 1737 | ±40 | 1746 | ±35 | 1834 | ±9 | 2355 | ±100 | +5 | 0.0194 | 216.8 | 3.207 | 2.3 | 0.1121 | 0.48 | 4.82 | 2.3 | 0.3118 | 2.3 | 0.98 |
| B.1.1 | – | – | 0.1133 | 0.73 | 0.260 | 0.8 | 1.161 | 1.2 | 0.33 | 0.69 | 1.5 | 1800 | ±44 | 1791 | ±50 | 1748 | ±49 | 1853 | ±13 | 2329 | ±72 | +3 | 0.1171 | 4.9 | 3.105 | 2.8 | 0.1133 | 0.73 | 5.03 | 2.9 | 0.3220 | 2.8 | 0.97 |
| B.23.1 | 7.1E-5 | 30 | 0.1127 | 0.51 | 0.018 | 2.0 | 1.276 | 1.6 | 0.20 | 0.05 | 1.2 | 1761 | ±36 | 1751 | ±41 | 1760 | ±36 | 1828 | ±11 | 1926 | ±120 | +4 | 0.0113 | 417.4 | 3.184 | 2.3 | 0.1117 | 0.58 | 4.84 | 2.4 | 0.3141 | 2.3 | 0.97 |
| B.20.1 | 9.2E-5 | 45 | 0.1130 | 0.83 | 0.155 | 1.2 | 1.126 | 1.3 | 0.18 | 0.42 | 1.6 | 1784 | ±45 | 1778 | ±52 | 1760 | ±48 | 1829 | ±18 | 2216 | ±77 | +3 | 0.1092 | 7.4 | 3.136 | 2.9 | 0.1118 | 0.98 | 4.92 | 3.1 | 0.3189 | 2.9 | 0.95 |
| B.19.1 | 3.2E-5 | 45 | 0.1141 | 0.51 | 0.180 | 1.4 | 1.154 | 0.9 | 0.23 | 0.47 | 1.2 | 1795 | ±37 | 1785 | ±42 | 1760 | ±40 | 1859 | ±10 | 2328 | ±66 | +4 | 0.1132 | 5.4 | 3.115 | 2.4 | 0.1137 | 0.54 | 5.03 | 2.4 | 0.3210 | 2.4 | 0.97 |
| B.45.1 | 8.7E-6 | 100 | 0.1145 | 0.58 | 0.140 | 1.6 | 1.199 | 2.3 | 0.14 | 0.39 | 1.3 | 1785 | ±39 | 1773 | ±44 | 1764 | ±41 | 1870 | ±11 | 2197 | ±68 | +5 | 0.1008 | 7.2 | 3.134 | 2.5 | 0.1144 | 0.59 | 5.03 | 2.6 | 0.3191 | 2.5 | 0.97 |
| B.44.1 | -8.9E-6 | 100 | 0.1132 | 0.59 | 0.110 | 1.7 | 1.213 | 1.0 | 0.12 | 0.30 | 1.4 | 1783 | ±40 | 1772 | ±45 | 1764 | ±42 | 1854 | ±11 | 2248 | ±71 | +4 | 0.1026 | 9.0 | 3.139 | 2.6 | 0.1133 | 0.60 | 4.98 | 2.6 | 0.3186 | 2.6 | 0.97 |
| B.26.1 | 3.8E-5 | 71 | 0.1059 | 0.85 | 0.184 | 1.2 | 1.000 | 0.7 | 0.17 | 0.52 | 1.5 | 1794 | ±42 | 1805 | ±49 | 1768 | ±46 | 1721 | ±17 | 2155 | ±69 | -5 | 0.1211 | 5.7 | 3.117 | 2.7 | 0.1054 | 0.93 | 4.66 | 2.8 | 0.3209 | 2.7 | 0.95 |
| B.24.1 | 1.4E-4 | 45 | 0.1127 | 1.01 | 0.232 | 1.2 | 1.196 | 1.5 | 0.26 | 0.63 | 1.8 | 1808 | ±50 | 1807 | ±58 | 1771 | ±55 | 1813 | ±23 | 2225 | ±84 | +0 | 0.1159 | 6.2 | 3.089 | 3.2 | 0.1108 | 1.29 | 4.95 | 3.4 | 0.3238 | 3.2 | 0.93 |
| B.36.1 | — | — | 0.1098 | 0.43 | 0.017 | 1.6 | 1.118 | 0.8 | 0.16 | 0.05 | 1.2 | 1785 | ±35 | 1784 | ±40 | 1783 | ±35 | 1796 | ±8 | 2200 | ±63 | +1 | 0.1002 | 47.5 | 3.134 | 2.2 | 0.1098 | 0.43 | 4.83 | 2.3 | 0.3191 | 2.2 | 0.98 |
| B.17.1 | 9.6E-5 | 38 | 0.1122 | 0.72 | 0.321 | 0.8 | 1.149 | 1.1 | 0.38 | 0.87 | 1.5 | 1842 | ±41 | 1847 | ±48 | 1784 | ±48 | 1814 | ±16 | 2305 | ±67 | -2 | 0.1230 | 4.2 | 3.023 | 2.6 | 0.1109 | 0.86 | 5.06 | 2.7 | 0.3308 | 2.6 | 0.95 |
| B.25.1 | 1.6E-4 | 38 | 0.1104 | 0.92 | 0.161 | 1.3 | 1.115 | 1.4 | 0.18 | 0.44 | 1.7 | 1816 | ±46 | 1823 | ±53 | 1793 | ±49 | 1771 | ±22 | 2205 | ±81 | -3 | 0.1219 | 7.1 | 3.073 | 2.9 | 0.1083 | 1.21 | 4.86 | 3.1 | 0.3254 | 2.9 | 0.92 |
| B.42.1 | 6.9E-5 | 58 | 0.1120 | 0.92 | 0.194 | 1.2 | 1.205 | 1.4 | 0.22 | 0.53 | 1.7 | 1828 | ±47 | 1829 | ±55 | 1795 | ±51 | 1818 | ±19 | 2282 | ±80 | -1 | 0.1208 | 6.5 | 3.050 | 3.0 | 0.1111 | 1.05 | 5.02 | 3.1 | 0.3278 | 3.0 | 0.94 |
| B.43.1 | -1.6E-5 | 100 | 0.1142 | 0.76 | 0.213 | 1.0 | 1.175 | 1.2 | 0.24 | 0.58 | 1.5 | 1846 | ±43 | 1842 | ±50 | 1807 | ±47 | 1871 | ±14 | 2320 | ±71 | +2 | 0.1186 | 5.6 | 3.016 | 2.7 | 0.1145 | 0.78 | 5.23 | 2.8 | 0.3315 | 2.7 | 0.96 |
| B.30.1 | 1.7E-5 | 50 | 0.1108 | 0.44 | 0.024 | 4.4 | 1.169 | 0.8 | 0.01 | 0.08 | 1.1 | 1810 | ±36 | 1811 | ±41 | 1809 | ±36 | 1808 | ±8 | 1959 | ±98 | -0 | 0.1035 | 31.0 | 3.084 | 2.3 | 0.1106 | 0.45 | 4.94 | 2.3 | 0.3243 | 2.3 | 0.98 |
| B.7.1 | 3.0E-5 | 50 | 0.1122 | 0.60 | 0.067 | 3.7 | 1.218 | 1.0 | 0.08 | 0.18 | 0.6 | 1821 | ±41 | 1820 | ±47 | 1810 | ±42 | 1829 | ±11 | 2324 | ±102 | +0 | 0.1190 | 14.2 | 3.063 | 2.6 | 0.1118 | 0.63 | 5.03 | 2.7 | 0.3265 | 2.6 | 0.97 |
| B.2.1 | 1.7E-5 | 100 | 0.1131 | 0.81 | 0.190 | 1.1 | 1.150 | 1.3 | 0.25 | 0.49 | 1.6 | 1860 | ±45 | 1862 | ±52 | 1820 | ±49 | 1846 | ±15 | 2439 | ±78 | -1 | 0.1301 | 6.3 | 2.991 | 2.8 | 0.1129 | 0.84 | 5.20 | 2.9 | 0.3344 | 2.8 | 0.96 |
| B.28.1 | 8.6E-5 | 35 | 0.1128 | 2.95 | 0.158 | 0.9 | 1.190 | 1.9 | 0.17 | 0.44 | 1.4 | 1845 | ±40 | 1848 | ±47 | 1821 | ±42 | 1826 | ±55 | 2255 | ±66 | -1 | 0.1211 | 9.2 | 3.018 | 2.5 | 0.1116 | 3.01 | 5.10 | 3.9 | 0.3314 | 2.5 | 0.63 |
| B.21.1 | 3.7E-5 | 71 | 0.1130 | 0.83 | 0.213 | 1.0 | 1.093 | 0.8 | 0.23 | 0.58 | 1.6 | 1858 | ±46 | 1861 | ±54 | 1822 | ±51 | 1839 | ±16 | 2309 | ±76 | -1 | 0.1233 | 6.0 | 2.993 | 2.9 | 0.1125 | 0.89 | 5.18 | 3.0 | 0.3341 | 2.9 | 0.96 |
| B.22.1 | 2.6E-5 | 100 | 0.1109 | 1.16 | 0.205 | 1.4 | 1.175 | 1.6 | 0.24 | 0.55 | 2.2 | 1861 | ±55 | 1869 | ±64 | 1823 | ±60 | 1808 | ±22 | 2354 | ±95 | -3 | 0.1300 | 7.3 | 2.989 | 3.4 | 0.1105 | 1.21 | 5.10 | 3.6 | 0.3346 | 3.4 | 0.94 |
| B.10.1 | 2.0E-5 | 100 | 0.1140 | 0.86 | 0.181 | 1.1 | 1.207 | 1.3 | 0.20 | 0.49 | 1.6 | 1858 | ±46 | 1858 | ±54 | 1825 | ±50 | 1860 | ±16 | 2338 | ±77 | +0 | 0.1223 | 6.7 | 2.994 | 2.8 | 0.1137 | 0.89 | 5.24 | 3.0 | 0.3340 | 2.8 | 0.95 |
| B.29.1 | -4.4E-5 | 58 | 0.1153 | 1.41 | 0.215 | 1.9 | 1.168 | 1.2 | 0.26 | 0.57 | 1.5 | 1872 | ±43 | 1868 | ±50 | 1828 | ±47 | 1894 | ±26 | 2431 | ±83 | +1 | 0.1250 | 6.2 | 2.968 | 2.6 | 0.1159 | 1.43 | 5.39 | 3.0 | 0.3369 | 2.6 | 0.88 |
| B.6.1 | 2.2E-5 | 100 | 0.1098 | 0.90 | 0.098 | 1.6 | 1.157 | 2.5 | 0.11 | 0.26 | 1.7 | 1846 | ±46 | 1855 | ±53 | 1829 | ±47 | 1791 | ±17 | 2329 | ±83 | -4 | 0.1361 | 10.2 | 3.015 | 2.8 | 0.1095 | 0.94 | 5.01 | 3.0 | 0.3316 | 2.8 | 0.95 |
| B.3.1 | -1.0E-5 | 100 | 0.1125 | 0.63 | 0.101 | 1.1 | 1.050 | 0.6 | 0.12 | 0.27 | 1.4 | 1850 | ±40 | 1851 | ±46 | 1830 | ±41 | 1843 | ±12 | 2399 | ±69 | -0 | 0.1278 | 9.0 | 3.009 | 2.5 | 0.1126 | 0.65 | 5.16 | 2.6 | 0.3323 | 2.5 | 0.97 |
| B.16.1 | — | — | 0.1122 | 0.98 | 0.176 | 1.3 | 1.192 | 1.5 | 0.20 | 0.48 | 1.8 | 1867 | ±50 | 1872 | ±59 | 1835 | ±54 | 1836 | ±18 | 2351 | ±84 | -2 | 0.1279 | 7.4 | 2.977 | 3.1 | 0.1122 | 0.98 | 5.20 | 3.2 | 0.3359 | 3.1 | 0.95 |
| B.34.1 | 1.9E-5 | 100 | 0.1133 | 1.67 | 0.157 | 3.3 | 1.142 | 3.5 | 0.18 | 0.42 | 1.6 | 1868 | ±23 | 1872 | ±27 | 1839 | ±25 | 1850 | ±31 | 2381 | ±89 | -1 | 0.1282 | 6.3 | 2.974 | 1.4 | 0.1131 | 1.69 | 5.24 | 2.2 | 0.3362 | 1.4 | 0.64 |
| B.32.1 | -3.4E-5 | 58 | 0.1114 | 0.66 | 0.108 | 1.1 | 1.212 | 1.1 | 0.11 | 0.30 | 1.4 | 1859 | ±41 | 1864 | ±48 | 1841 | ±43 | 1830 | ±13 | 2309 | ±69 | -2 | 0.1277 | 8.5 | 2.992 | 2.5 | 0.1119 | 0.70 | 5.16 | 2.6 | 0.3343 | 2.5 | 0.96 |
| B.35.1 | 1.3E-5 | 100 | 0.1163 | 2.08 | 0.204 | 0.9 | 1.114 | 0.7 | 0.25 | 0.54 | 1.4 | 1885 | ±42 | 1882 | ±50 | 1844 | ±46 | 1898 | ±38 | 2421 | ±71 | +1 | 0.1255 | 6.9 | 2.945 | 2.6 | 0.1162 | 2.09 | 5.44 | 3.3 | 0.3396 | 2.6 | 0.78 |
| B.38.1 | 3.2E-5 | 22 | 0.1112 | 0.31 | 0.013 | 1.2 | 1.470 | 0.7 | 0.03 | 0.02 | 1.1 | 1849 | ±34 | 1855 | ±39 | 1845 | ±34 | 1812 | ±6 | 3023 | ±100 | -2 | 0.2693 | 37.1 | 3.010 | 2.1 | 0.1107 | 0.32 | 5.07 | 2.1 | 0.3322 | 2.1 | 0.99 |
| B.12.1 | 2.0E-5 | 71 | 0.1139 | 0.63 | 0.111 | 1.1 | 1.151 | 1.0 | 0.11 | 0.31 | 1.3 | 1864 | ±39 | 1865 | ±46 | 1846 | ±41 | 1858 | ±12 | 2300 | ±65 | -0 | 0.1218 | 8.4 | 2.982 | 2.4 | 0.1136 | 0.65 | 5.25 | 2.5 | 0.3353 | 2.4 | 0.97 |
| B.27.1 | -6.4E-5 | 50 | 0.1115 | 0.78 | 0.185 | 1.0 | 1.235 | 1.2 | 0.20 | 0.51 | 1.5 | 1888 | ±44 | 1896 | ±52 | 1853 | ±47 | 1839 | ±16 | 2392 | ±75 | -3 | 0.1327 | 6.1 | 2.939 | 2.7 | 0.1124 | 0.87 | 5.27 | 2.8 | 0.3402 | 2.7 | 0.95 |
| B.5.1 | 4.9E-5 | 58 | 0.1103 | 0.78 | 0.081 | 1.5 | 1.176 | 1.2 | 0.08 | 0.22 | 1.5 | 1865 | ±44 | 1876 | ±51 | 1853 | ±45 | 1794 | ±16 | 2268 | ±80 | -5 | 0.1408 | 11.2 | 2.981 | 2.7 | 0.1097 | 0.86 | 5.07 | 2.8 | 0.3354 | 2.7 | 0.95 |
| B.39.1 | -2.0E-5 | 100 | 0.1141 | 0.85 | 0.193 | 1.1 | 1.163 | 1.3 | 0.21 | 0.53 | 1.6 | 1895 | ±46 | 1900 | ±55 | 1859 | ±50 | 1870 | ±16 | 2392 | ±78 | -2 | 0.1291 | 6.5 | 2.926 | 2.8 | 0.1144 | 0.87 | 5.39 | 3.0 | 0.3418 | 2.8 | 0.96 |
| B.33.1 | — | — | 0.1119 | 0.79 | 0.184 | 1.1 | 1.189 | 1.3 | 0.19 | 0.51 | 1.6 | 1896 | ±45 | 1907 | ±53 | 1864 | ±49 | 1830 | ±14 | 2348 | ±74 | -4 | 0.1326 | 6.3 | 2.925 | 2.7 | 0.1119 | 0.79 | 5.27 | 2.8 | 0.3419 | 2.7 | 0.96 |
| B.9.1 | 1.9E-5 | 100 | 0.1138 | 0.83 | 0.213 | 1.0 | 0.987 | 0.6 | 0.26 | 0.57 | 1.5 | 1908 | ±45 | 1917 | ±53 | 1866 | ±49 | 1858 | ±16 | 2441 | ±76 | -3 | 0.1350 | 5.8 | 2.903 | 2.7 | 0.1136 | 0.86 | 5.39 | 2.9 | 0.3445 | 2.7 | 0.95 |
| B.11.1 | 3.3E-5 | 71 | 0.1134 | 0.78 | 0.110 | 1.3 | 1.130 | 0.6 | 0.12 | 0.30 | 1.5 | 1906 | ±45 | 1916 | ±53 | 1887 | ±47 | 1848 | ±15 | 2401 | ±79 | -4 | 0.1408 | 9.4 | 2.906 | 2.7 | 0.1130 | 0.83 | 5.36 | 2.8 | 0.3441 | 2.7 | 0.96 |
| B.37.1 | -8.7E-5 | 45 | 0.1127 | 0.89 | 0.186 | 1.1 | 1.155 | 1.2 | 0.20 | 0.51 | 1.6 | 1930 | ±45 | 1943 | ±54 | 1894 | ±49 | 1862 | ±18 | 2452 | ±79 | -4 | 0.1392 | 6.4 | 2.864 | 2.7 | 0.1139 | 1.00 | 5.48 | 2.9 | 0.3491 | 2.7 | 0.94 |
| B.4.1 | -8.0E-5 | 50 | 0.1167 | 2.46 | 0.162 | 1.3 | 1.274 | 4.9 | 0.17 | 0.45 | 1.6 | 2144 | ±49 | 2195 | ±64 | 2110 | ±53 | 1922 | ±44 | 2705 | ±89 | -14 | 0.1938 | 9.2 | 2.534 | 2.7 | 0.1178 | 2.48 | 6.41 | 3.7 | 0.3946 | 2.7 | 0.74 |

Errors are 1-sigma; Pbc and Pb* indicate the common and radiogenic portions. respectively. Error in Standard calibration was 0.64% (not included in above errors but required when comparing data from different mounts). (1) Common Pb corrected using measured 204Pb. (2) Common Pb corrected by assuming 206Pb/238U-207Pb/235U age-concordance. (3) Common Pb corrected by assuming 206Pb/238U-208Pb/232Th age-concordance

**Łanowicze 1405**

| Spot | $^{204}Pb/^{206}Pb$ | ±% | $^{207}Pb/^{206}Pb$ | ±% | $^{208}Pb/^{206}Pb$ | ±% | $^{206}Pb/^{238}U$ | ±% | % $^{206}Pbc$ | $^{232}Th/^{238}U$ | ±% | (1) $^{206}Pb/^{238}U$ | Age | (2) $^{206}Pb/^{238}U$ | Age | (3) $^{206}Pb/^{238}U$ | Age | (1)$^{207}Pb/^{206}Pb$ | Age | (1) 208Pb/232Th | Age | % Discordant | (1) $^{238}U/^{206}Pb$* | ±% | (1) $^{207}Pb*/^{206}Pb*$ | ±% | (1) $^{207}Pb*/^{235}U$ | ±% | (1) $^{206}Pb*/^{238}U$ | ±% | errcorr |
|---|---|---|---|---|---|---|---|---|---|---|---|---|---|---|---|---|---|---|---|---|---|---|---|---|---|---|---|---|---|---|---|
| LAN-16.1 | -5.1E-6 | 71 | 0.1015 | 0.72 | 0.061 | 4.0 | 0.721 | 1.00 | – | 0.16 | 0.72 | 1655 | ±41 | 1656 | ±46 | 1645 | ±42 | 1653 | ±13 | 2120 | ±100 | -0 | 3.42 | 2.8 | 0.1016 | 0.72 | 4.10 | 2.9 | 0.293 | 2.8 | 0.969 |
| LAN-6.1 | 2.2E-5 | 33 | 0.1103 | 0.37 | 0.107 | 0.7 | 0.829 | 0.51 | 0.04 | 0.37 | 0.50 | 1759 | ±42 | 1753 | ±48 | 1759 | ±45 | 1799 | ±7 | 1746 | ±49 | +3 | 3.19 | 2.8 | 0.1100 | 0.39 | 4.76 | 2.8 | 0.314 | 2.8 | 0.990 |
| LAN-4.1 | 3.2E-5 | 35 | 0.1137 | 0.88 | 0.151 | 2.1 | 0.769 | 0.39 | 0.08 | 0.54 | 0.63 | 1830 | ±74 | 1827 | ±86 | 1836 | ±80 | 1850 | ±16 | 1756 | ±87 | +1 | 3.05 | 4.7 | 0.1131 | 0.90 | 5.12 | 4.7 | 0.328 | 4.7 | 0.982 |
| LAN-20.1 | 2.3E-5 | 50 | 0.1131 | 0.48 | 0.199 | 0.7 | 0.703 | 0.40 | 0.02 | 0.69 | 0.52 | 1833 | ±44 | 1831 | ±51 | 1833 | ±49 | 1848 | ±9 | 1836 | ±51 | +1 | 3.04 | 2.8 | 0.1130 | 0.49 | 5.12 | 2.8 | 0.329 | 2.8 | 0.985 |
| LAN-7.1 | 6.7E-5 | 29 | 0.1128 | 0.51 | 0.157 | 0.8 | 0.695 | 0.42 | 0.08 | 0.54 | 0.59 | 1834 | ±59 | 1834 | ±68 | 1834 | ±64 | 1836 | ±10 | 1833 | ±67 | +0 | 3.04 | 3.7 | 0.1122 | 0.54 | 5.09 | 3.7 | 0.329 | 3.7 | 0.990 |
| LAN-8.1 | 4.8E-5 | 28 | 0.1127 | 1.44 | 0.097 | 2.1 | 0.746 | 2.44 | 0.09 | 0.31 | 1.08 | 1835 | ±46 | 1835 | ±53 | 1830 | ±48 | 1833 | ±26 | 1958 | ±70 | -0 | 3.04 | 2.9 | 0.1121 | 1.46 | 5.09 | 3.2 | 0.329 | 2.9 | 0.892 |
| LAN-5.1 | 6.9E-5 | 24 | 0.1109 | 0.48 | 0.107 | 0.9 | 0.826 | 1.32 | 0.06 | 0.35 | 0.65 | 1838 | ±46 | 1842 | ±54 | 1834 | ±49 | 1808 | ±9 | 1924 | ±57 | -2 | 3.03 | 2.9 | 0.1105 | 0.50 | 5.03 | 2.9 | 0.330 | 2.9 | 0.986 |
| LAN-2.1 | 4.1E-5 | 33 | 0.1128 | 0.37 | 0.031 | 1.3 | 0.857 | 0.91 | 0.06 | 0.11 | 0.88 | 1841 | ±50 | 1841 | ±58 | 1842 | ±51 | 1838 | ±7 | 1728 | ±62 | -0 | 3.03 | 3.1 | 0.1124 | 0.39 | 5.12 | 3.2 | 0.331 | 3.1 | 0.992 |
| LAN-11.1 | 3.5E-5 | 27 | 0.1128 | 0.50 | 0.194 | 1.3 | 0.846 | 3.22 | 0.02 | 0.67 | 0.56 | 1843 | ±71 | 1843 | ±82 | 1843 | ±78 | 1843 | ±9 | 1838 | ±82 | -0 | 3.02 | 4.4 | 0.1127 | 0.51 | 5.14 | 4.5 | 0.331 | 4.4 | 0.994 |
| LAN-15.1 | 9.0E-6 | 71 | 0.1140 | 0.65 | 0.180 | 2.3 | 0.733 | 0.53 | 0.07 | 0.62 | 0.73 | 1851 | ±49 | 1850 | ±57 | 1852 | ±54 | 1855 | ±12 | 1841 | ±68 | +0 | 3.01 | 3.1 | 0.1135 | 0.68 | 5.20 | 3.1 | 0.333 | 3.1 | 0.976 |
| LAN-3.1 | 2.0E-5 | 41 | 0.1131 | 2.13 | 0.136 | 0.8 | 0.737 | 0.34 | 0.13 | 0.48 | 0.58 | 1858 | ±53 | 1861 | ±61 | 1862 | ±56 | 1835 | ±39 | 1792 | ±59 | -1 | 2.99 | 3.3 | 0.1122 | 2.16 | 5.17 | 3.9 | 0.334 | 3.3 | 0.834 |
| LAN-14.1 | 8.3E-6 | 71 | 0.1111 | 1.44 | 0.149 | 0.9 | 0.852 | 0.80 | 0.04 | 0.51 | 0.68 | 1862 | ±48 | 1869 | ±56 | 1862 | ±52 | 1813 | ±26 | 1859 | ±57 | -3 | 2.99 | 3.0 | 0.1108 | 1.46 | 5.12 | 3.3 | 0.335 | 3.0 | 0.899 |
| LAN-10.1 | 5.7E-5 | 32 | 0.1139 | 0.57 | 0.152 | 1.8 | 0.800 | 2.38 | 0.11 | 0.48 | 2.04 | 1865 | ±56 | 1867 | ±65 | 1855 | ±60 | 1850 | ±11 | 2009 | ±85 | -1 | 2.98 | 3.4 | 0.1131 | 0.61 | 5.23 | 3.5 | 0.335 | 3.4 | 0.984 |
| LAN-1.1 | 4.5E-5 | 33 | 0.1130 | 0.43 | 0.065 | 1.7 | 0.876 | 0.62 | 0.04 | 0.23 | 0.76 | 1870 | ±47 | 1874 | ±54 | 1870 | ±48 | 1843 | ±8 | 1852 | ±62 | -2 | 2.97 | 2.9 | 0.1127 | 0.44 | 5.23 | 2.9 | 0.336 | 2.9 | 0.988 |
| LAN-9.1 | 3.0E-6 | 100 | 0.1132 | 0.81 | 0.229 | 1.2 | 0.887 | 1.17 | 0.01 | 0.80 | 0.84 | 1870 | ±54 | 1873 | ±63 | 1872 | ±61 | 1850 | ±15 | 1850 | ±64 | -1 | 2.97 | 3.3 | 0.1131 | 0.82 | 5.25 | 3.4 | 0.337 | 3.3 | 0.971 |
| LAN-13.1 | -4.3E-6 | 100 | 0.1124 | 0.56 | 0.153 | 1.5 | 0.814 | 0.76 | 0.12 | 0.52 | 0.66 | 1879 | ±57 | 1888 | ±66 | 1878 | ±61 | 1823 | ±11 | 1890 | ±70 | -4 | 2.96 | 3.5 | 0.1115 | 0.61 | 5.20 | 3.5 | 0.338 | 3.5 | 0.985 |
| LAN-19.1 | 1.3E-5 | 71 | 0.1148 | 1.58 | 0.171 | 0.7 | 0.821 | 2.00 | 0.03 | 0.58 | 0.49 | 1905 | ±54 | 1910 | ±64 | 1902 | ±59 | 1874 | ±29 | 1939 | ±63 | -2 | 2.91 | 3.3 | 0.1146 | 1.58 | 5.43 | 3.7 | 0.344 | 3.3 | 0.902 |
| LAN-18.1 | 3.7E-5 | 45 | 0.1136 | 0.62 | 0.155 | 2.3 | 0.802 | 1.53 | 0.02 | 0.50 | 0.72 | 1913 | ±49 | 1922 | ±58 | 1904 | ±53 | 1855 | ±11 | 2042 | ±75 | -4 | 2.90 | 3.0 | 0.1134 | 0.63 | 5.40 | 3.1 | 0.345 | 3.0 | 0.978 |
| LAN-12.1 | 1.6E-5 | 45 | 0.1134 | 0.49 | 0.170 | 1.6 | 0.850 | 0.69 | – | 0.59 | 0.56 | 1915 | ±48 | 1925 | ±57 | 1915 | ±52 | 1855 | ±9 | 1916 | ±62 | -4 | 2.89 | 2.9 | 0.1134 | 0.49 | 5.41 | 3.0 | 0.346 | 2.9 | 0.986 |
| LAN-22.1 | -1.5E-5 | 58 | 0.1084 | 0.88 | 0.178 | 0.79 | 0.772 | 1.30 | – | 0.63 | 1.02 | 1784 | ±18 | 1785 | ±21 | 1788 | ±20 | 1776 | ±16 | 1745 | ±29 | -1 | 3.136 | 1.2 | 0.1086 | 0.89 | 4.78 | 1.5 | 0.3189 | 1.2 | 0.80 |
| LAN-21.1 | 4.8E-5 | 32 | 0.1129 | 0.53 | 0.171 | 1.35 | 0.745 | 2.74 | 0.09 | 0.65 | 0.53 | 1785 | ±38 | 1778 | ±43 | 1801 | ±41 | 1836 | ±10 | 1608 | ±44 | +3 | 3.134 | 2.4 | 0.1123 | 0.57 | 4.94 | 2.5 | 0.3191 | 2.4 | 0.97 |
| LAN-27.1 | -1.3E-5 | 71 | 0.1123 | 2.23 | 0.139 | 1.03 | 0.759 | 0.83 | – | 0.49 | 0.72 | 1798 | ±21 | 1792 | ±25 | 1800 | ±23 | 1839 | ±40 | 1774 | ±32 | +3 | 3.108 | 1.4 | 0.1124 | 2.23 | 4.99 | 2.6 | 0.3217 | 1.4 | 0.52 |
| LAN-23.1 | 1.6E-5 | 53 | 0.1128 | 0.50 | 0.121 | 0.91 | 0.839 | 0.71 | 0.03 | 0.44 | 0.64 | 1819 | ±19 | 1815 | ±21 | 1823 | ±20 | 1841 | ±9 | 1739 | ±27 | +1 | 3.068 | 1.2 | 0.1126 | 0.51 | 5.06 | 1.3 | 0.3259 | 1.2 | 0.92 |
| LAN-28.1 | 1.3E-4 | 24 | 0.1143 | 0.63 | 0.214 | 0.89 | 0.783 | 0.91 | 0.24 | 0.73 | 0.68 | 1831 | ±23 | 1830 | ±26 | 1831 | ±25 | 1842 | ±13 | 1833 | ±33 | +1 | 3.043 | 1.4 | 0.1126 | 0.74 | 5.10 | 1.6 | 0.3286 | 1.4 | 0.89 |
| LAN-25.1 | 1.6E-5 | 53 | 0.1132 | 1.26 | 0.137 | 0.94 | 0.793 | 0.74 | 0.07 | 0.48 | 0.67 | 1801 | ±11 | 1795 | ±14 | 1803 | ±12 | 1843 | ±23 | 1768 | ±24 | +3 | 3.102 | 0.7 | 0.1127 | 1.28 | 5.01 | 1.5 | 0.3224 | 0.7 | 0.50 |
| LAN-26.1 | 2.4E-5 | 50 | 0.1140 | 0.58 | 0.194 | 0.86 | 0.809 | 0.79 | 0.04 | 0.67 | 0.63 | 1865 | ±21 | 1866 | ±25 | 1864 | ±23 | 1859 | ±11 | 1871 | ±30 | -0 | 2.981 | 1.3 | 0.1137 | 0.60 | 5.26 | 1.4 | 0.3355 | 1.3 | 0.91 |
| LAN-29.1 | 5.9E-6 | 41 | 0.1181 | 0.23 | 0.223 | 0.97 | 0.861 | 1.61 | 0.01 | 0.79 | 0.82 | 1922 | ±12 | 1921 | ±14 | 1926 | ±13 | 1926 | ±4 | 1879 | ±26 | +0 | 2.880 | 0.7 | 0.1180 | 0.23 | 5.65 | 0.7 | 0.3473 | 0.7 | 0.95 |

Errors are 1-sigma; Pbc and Pb* indicate the common and radiogenic portions. respectively. Error in Standard calibration was 0.27% (not included in above errors but required when comparing data from different mounts). (1) Common Pb corrected using measured 204Pb. (2) Common Pb corrected by assuming 206Pb/238U-207Pb/235U age-concordance. (2) Common Pb corrected by assuming 206Pb/238U-207Pb/235U age-concordance. (3) Common Pb corrected by assuming 206Pb/238U-208Pb/232Th age-concordance

**Łanowicze 1485**

| Spot | $^{204}Pb/^{206}Pb$ | ±% | $^{207}Pb/^{206}Pb$ | ±% | $^{208}Pb/^{206}Pb$ | ±% | $^{206}Pb/^{238}U$ | ±% | % $^{206}Pbc$ | $^{232}Th/^{238}U$ | ±% | (1) $^{206}Pb/^{238}U$ | Age | (2) $_{206}Pb/^{238}U$ | Age | (3) $^{206}Pb/^{238}U$ | Age | (1) $^{207}Pb/^{206}Pb$ | Age | (1) $^{208}Pb/^{232}Th$ | Age | % Discordant | 7corr $^{208}Pb*/^{232}Th$ | ±% | (1) $^{238}U/^{206}Pb*$ | ±% | (1) $^{207}Pb*/^{206}Pb*$ | ±% | (1) $^{207}Pb*/^{235}U$ | ±% | (1) $^{206}Pb*/^{238}U$ | ±% | errcorr |
|---|---|---|---|---|---|---|---|---|---|---|---|---|---|---|---|---|---|---|---|---|---|---|---|---|---|---|---|---|---|---|---|---|
| C.39.1 | -5.2E-4 | 14 | 0.0943 | 0.67 | 0.031 | 2.0 | 0.864 | 0.40 | – | 0.08 | 0.89 | 1440 | ±53 | 1420 | ±57 | 1424 | ±53 | 1649 | ±22 | 2895 | ±197 | +14 | 0.056 | 42 | 3.994 | 4.1 | 0.1014 | 1.2 | 3.50 | 4.3 | 0.2504 | 4.1 | 0.96 |
| C.8.1 | -3.3E-4 | 15 | 0.0951 | 0.55 | 0.026 | 1.8 | 0.880 | 0.67 | – | 0.07 | 0.77 | 1465 | ±51 | 1450 | ±55 | 1453 | ±51 | 1618 | ±16 | 2702 | ±165 | +11 | 0.055 | 51 | 3.919 | 3.9 | 0.0997 | 0.8 | 3.51 | 4.0 | 0.2552 | 3.9 | 0.98 |
| C.37.1 | -2.8E-4 | 15 | 0.0961 | 0.51 | 0.019 | 2.0 | 0.936 | 0.63 | – | 0.05 | 1.27 | 1485 | ±53 | 1471 | ±58 | 1475 | ±53 | 1625 | ±14 | 2977 | ±197 | +10 | 0.042 | 101 | 3.859 | 4.0 | 0.1000 | 0.7 | 3.57 | 4.1 | 0.2591 | 4.0 | 0.98 |
| C.42.1 | -4.2E-4 | 14 | 0.0935 | 0.59 | 0.027 | 1.9 | 0.931 | 0.71 | – | 0.07 | 0.79 | 1489 | ±54 | 1477 | ±59 | 1475 | ±54 | 1611 | ±18 | 2880 | ±185 | +8 | 0.085 | 34 | 3.848 | 4.1 | 0.0993 | 1.0 | 3.56 | 4.2 | 0.2599 | 4.1 | 0.97 |
| C.27.1 | -1.2E-3 | 11 | 0.0958 | 0.76 | 0.039 | 2.0 | 0.880 | 0.93 | – | 0.10 | 1.00 | 1492 | ±55 | 1456 | ±59 | 1458 | ±55 | 1822 | ±29 | 3896 | ±265 | +20 | 0.069 | 31 | 3.839 | 4.2 | 0.1114 | 1.6 | 4.00 | 4.5 | 0.2605 | 4.2 | 0.93 |
| C.2.2 | -2.0E-4 | 18 | 0.1052 | 0.50 | 0.033 | 1.5 | 0.889 | 0.40 | – | 0.09 | 0.74 | 1623 | ±58 | 1605 | ±64 | 1612 | ±58 | 1764 | ±12 | 2565 | ±133 | +9 | 0.053 | 61 | 3.494 | 4.0 | 0.1079 | 0.7 | 4.26 | 4.1 | 0.2862 | 4.0 | 0.99 |
| C.40.1 | -5.6E-5 | 31 | 0.1122 | 0.44 | 0.162 | 2.7 | 1.043 | 0.62 | – | 0.48 | 0.68 | 1666 | ±59 | 1642 | ±65 | 1647 | ±63 | 1847 | ±9 | 1952 | ±92 | +11 | 0.081 | 9 | 3.391 | 4.0 | 0.1129 | 0.5 | 4.59 | 4.0 | 0.2949 | 4.0 | 0.99 |
| C.30.1 | -2.8E-4 | 12 | 0.1117 | 0.60 | 0.110 | 2.3 | 1.097 | 0.53 | – | 0.30 | 0.58 | 1713 | ±59 | 1689 | ±65 | 1688 | ±61 | 1887 | ±12 | 2332 | ±103 | +10 | 0.088 | 13 | 3.285 | 3.9 | 0.1155 | 0.7 | 4.85 | 4.0 | 0.3044 | 3.9 | 0.98 |
| C.52.2 | -1.1E-4 | 16 | 0.1096 | 0.36 | 0.056 | 0.9 | 1.072 | 1.22 | – | 0.13 | 1.28 | 1714 | ±60 | 1700 | ±67 | 1698 | ±61 | 1819 | ±8 | 2629 | ±109 | +7 | 0.093 | 27 | 3.283 | 4.0 | 0.1112 | 0.4 | 4.67 | 4.0 | 0.3046 | 4.0 | 0.99 |
| C.50.1 | -2.0E-4 | 14 | 0.1116 | 0.37 | 0.097 | 3.9 | 1.229 | 0.57 | – | 0.29 | 0.62 | 1719 | ±60 | 1697 | ±67 | 1704 | ±63 | 1870 | ±9 | 2098 | ±114 | +9 | 0.079 | 16 | 3.273 | 4.0 | 0.1144 | 0.5 | 4.82 | 4.0 | 0.3056 | 4.0 | 0.99 |
| C.44.1 | -3.0E-4 | 14 | 0.1080 | 0.46 | 0.022 | 1.7 | 1.041 | 0.64 | – | 0.07 | 0.70 | 1726 | ±61 | 1711 | ±68 | 1716 | ±61 | 1833 | ±12 | 2882 | ±174 | +7 | 0.061 | 83 | 3.257 | 4.0 | 0.1120 | 0.7 | 4.74 | 4.1 | 0.3070 | 4.0 | 0.99 |
| C.20.1 | -1.5E-4 | 15 | 0.1117 | 0.62 | 0.026 | 2.2 | 1.163 | 0.54 | – | 0.07 | 0.61 | 1730 | ±61 | 1712 | ±68 | 1723 | ±61 | 1860 | ±12 | 2519 | ±127 | +8 | 0.028 | 167 | 3.248 | 4.0 | 0.1138 | 0.7 | 4.83 | 4.1 | 0.3079 | 4.0 | 0.99 |
| C.52.1 | -8.9E-5 | 19 | 0.1106 | 0.39 | 0.055 | 1.4 | 1.128 | 0.54 | – | 0.15 | 0.64 | 1734 | ±61 | 1720 | ±68 | 1723 | ±62 | 1830 | ±8 | 2251 | ±94 | +6 | 0.081 | 29 | 3.241 | 4.0 | 0.1118 | 0.4 | 4.76 | 4.0 | 0.3086 | 4.0 | 0.99 |
| C.13.1 | -2.2E-4 | 12 | 0.1124 | 0.60 | 0.285 | 2.7 | 1.145 | 0.94 | – | 0.70 | 1.39 | 1738 | ±61 | 1717 | ±68 | 1665 | ±68 | 1886 | ±12 | 2456 | ±116 | +9 | 0.116 | 7 | 3.232 | 4.0 | 0.1154 | 0.7 | 4.92 | 4.0 | 0.3094 | 4.0 | 0.99 |
| C.9.1 | -3.4E-4 | 13 | 0.1110 | 0.45 | 0.171 | 0.6 | 1.147 | 1.99 | – | 0.45 | 0.73 | 1744 | ±62 | 1723 | ±69 | 1704 | ±66 | 1888 | ±12 | 2385 | ±95 | +9 | 0.106 | 9 | 3.219 | 4.0 | 0.1155 | 0.7 | 4.95 | 4.1 | 0.3107 | 4.0 | 0.99 |
| C.6.2 | -2.4E-4 | 14 | 0.1101 | 0.85 | 0.015 | 3.1 | 1.003 | 0.34 | – | 0.04 | 0.67 | 1745 | ±61 | 1729 | ±69 | 1735 | ±61 | 1853 | ±16 | 3510 | ±234 | +7 | 0.026 | 346 | 3.217 | 4.0 | 0.1133 | 0.9 | 4.86 | 4.1 | 0.3108 | 4.0 | 0.97 |
| C.16.1 | -1.2E-3 | 10 | 0.1050 | 2.48 | 0.185 | 0.9 | 1.053 | 0.88 | – | 0.51 | 0.97 | 1745 | ±63 | 1712 | ±71 | 1683 | ±67 | 1969 | ±44 | 2614 | ±118 | +13 | 0.110 | 9 | 3.216 | 4.2 | 0.1208 | 2.5 | 5.18 | 4.8 | 0.3109 | 4.2 | 0.86 |
| C.4.1 | -8.1E-5 | 18 | 0.1117 | 0.32 | 0.113 | 0.6 | 1.123 | 0.47 | – | 0.34 | 0.55 | 1746 | ±61 | 1732 | ±68 | 1733 | ±63 | 1844 | ±7 | 2025 | ±78 | +6 | 0.088 | 12 | 3.215 | 4.0 | 0.1128 | 0.4 | 4.84 | 4.0 | 0.3110 | 4.0 | 1.00 |
| C.10.1 | -2.0E-4 | 15 | 0.1096 | 0.42 | 0.070 | 1.0 | 1.106 | 1.07 | – | 0.20 | 0.65 | 1747 | ±61 | 1734 | ±69 | 1733 | ±63 | 1838 | ±10 | 2271 | ±95 | +6 | 0.092 | 20 | 3.213 | 4.0 | 0.1123 | 0.5 | 4.82 | 4.0 | 0.3112 | 4.0 | 0.99 |
| C.25.2 | -4.9E-4 | 13 | 0.1129 | 0.56 | 0.075 | 1.1 | 1.113 | 0.78 | – | 0.20 | 1.50 | 1753 | ±63 | 1724 | ±70 | 1727 | ±64 | 1947 | ±16 | 2713 | ±133 | +11 | 0.083 | 22 | 3.200 | 4.1 | 0.1194 | 0.9 | 5.15 | 4.2 | 0.3125 | 4.1 | 0.98 |
| C.18.1 | -2.5E-4 | 13 | 0.1115 | 0.39 | 0.027 | 1.3 | 1.127 | 1.22 | – | 0.07 | 0.28 | 1754 | ±61 | 1736 | ±69 | 1742 | ±62 | 1879 | ±10 | 3025 | ±153 | +8 | 0.053 | 95 | 3.198 | 4.0 | 0.1149 | 0.5 | 4.96 | 4.0 | 0.3127 | 4.0 | 0.99 |
| C.38.1 | -3.2E-4 | 11 | 0.1114 | 0.63 | 0.015 | 1.7 | 1.061 | 1.70 | – | 0.04 | 0.28 | 1755 | ±61 | 1735 | ±69 | 1743 | ±61 | 1891 | ±13 | 3907 | ±231 | +8 | 0.000 | 32491 | 3.196 | 4.0 | 0.1157 | 0.7 | 4.99 | 4.0 | 0.3129 | 4.0 | 0.98 |
| C.51.2 | -7.6E-4 | 15 | 0.1103 | 2.39 | 0.198 | 1.0 | 1.037 | 1.08 | – | 0.53 | 1.18 | 1757 | ±66 | 1725 | ±74 | 1700 | ±71 | 1963 | ±45 | 2510 | ±118 | +12 | 0.107 | 9 | 3.192 | 4.3 | 0.1205 | 2.5 | 5.20 | 5.0 | 0.3133 | 4.3 | 0.86 |
| C.11.1 | -6.1E-5 | 20 | 0.1089 | 2.47 | 0.182 | 1.2 | 1.081 | 0.28 | – | 0.51 | 0.53 | 1762 | ±61 | 1758 | ±70 | 1733 | ±66 | 1795 | ±45 | 2169 | ±86 | +2 | 0.109 | 9 | 3.181 | 3.9 | 0.1097 | 2.5 | 4.76 | 4.6 | 0.3144 | 3.9 | 0.85 |
| C.45.1 | -2.6E-4 | 13 | 0.1111 | 0.91 | 0.052 | 6.6 | 1.078 | 0.60 | – | 0.14 | 0.43 | 1764 | ±62 | 1748 | ±70 | 1749 | ±63 | 1874 | ±17 | 2601 | ±196 | +7 | 0.089 | 31 | 3.176 | 4.0 | 0.1146 | 1.0 | 4.98 | 4.1 | 0.3148 | 4.0 | 0.97 |
| C.51.1 | -4.5E-4 | 15 | 0.1109 | 1.71 | 0.140 | 3.1 | 1.072 | 6.36 | – | 0.39 | 0.97 | 1765 | ±61 | 1744 | ±69 | 1732 | ±64 | 1911 | ±32 | 2392 | ±121 | +9 | 0.102 | 11 | 3.174 | 3.9 | 0.1170 | 1.8 | 5.08 | 4.3 | 0.3150 | 3.9 | 0.91 |
| C.34.1 | -3.1E-4 | 22 | 0.1142 | 1.34 | 0.140 | 1.1 | 1.074 | 0.53 | – | 0.38 | 1.18 | 1777 | ±67 | 1753 | ±75 | 1743 | ±70 | 1932 | ±27 | 2426 | ±113 | +9 | 0.101 | 12 | 3.152 | 4.3 | 0.1184 | 1.5 | 5.18 | 4.6 | 0.3173 | 4.3 | 0.94 |
| C.33.1 | -6.9E-4 | 13 | 0.1125 | 1.95 | 0.177 | 2.7 | 1.073 | 0.89 | – | 0.47 | 0.97 | 1779 | ±64 | 1747 | ±72 | 1726 | ±69 | 1981 | ±36 | 2580 | ±128 | +12 | 0.108 | 10 | 3.147 | 4.1 | 0.1217 | 2.0 | 5.33 | 4.6 | 0.3178 | 4.1 | 0.90 |
| C.29.1 | -6.2E-4 | 13 | 0.1093 | 0.60 | 0.119 | 4.3 | 0.970 | 0.49 | – | 0.36 | 2.25 | 1780 | ±61 | 1759 | ±69 | 1750 | ±64 | 1919 | ±19 | 2383 | ±148 | +8 | 0.100 | 12 | 3.145 | 3.9 | 0.1175 | 1.0 | 5.15 | 4.1 | 0.3180 | 3.9 | 0.97 |
| C.25.1 | -7.2E-4 | 15 | 0.1112 | 2.44 | 0.187 | 1.1 | 1.077 | 1.06 | – | 0.50 | 1.16 | 1781 | ±67 | 1752 | ±75 | 1728 | ±71 | 1969 | ±45 | 2535 | ±118 | +11 | 0.109 | 10 | 3.142 | 4.3 | 0.1208 | 2.5 | 5.30 | 5.0 | 0.3183 | 4.3 | 0.86 |
| C.28.1 | -5.1E-4 | 14 | 0.1089 | 0.61 | 0.101 | 4.3 | 1.086 | 0.84 | – | 0.32 | 0.83 | 1793 | ±64 | 1778 | ±73 | 1771 | ±67 | 1890 | ±18 | 2300 | ±140 | +6 | 0.100 | 14 | 3.119 | 4.1 | 0.1157 | 1.0 | 5.11 | 4.2 | 0.3206 | 4.1 | 0.97 |
| C.14.1 | -2.1E-4 | 14 | 0.1116 | 0.79 | 0.016 | 1.7 | 1.155 | 0.54 | – | 0.04 | 0.29 | 1794 | ±62 | 1783 | ±71 | 1786 | ±63 | 1871 | ±15 | 3217 | ±188 | +5 | 0.061 | 147 | 3.116 | 4.0 | 0.1144 | 0.8 | 5.06 | 4.1 | 0.3210 | 4.0 | 0.98 |
| C.48.1 | -3.3E-4 | 11 | 0.1121 | 0.65 | 0.015 | 1.7 | 1.044 | 0.28 | – | 0.04 | 0.29 | 1795 | ±63 | 1778 | ±71 | 1783 | ±63 | 1904 | ±14 | 4031 | ±243 | +7 | 0.046 | 203 | 3.114 | 4.0 | 0.1166 | 0.8 | 5.16 | 4.1 | 0.3212 | 4.0 | 0.98 |
| C.19.1 | -3.9E-4 | 11 | 0.1096 | 0.47 | 0.034 | 4.3 | 1.099 | 0.61 | – | 0.11 | 0.65 | 1797 | ±63 | 1785 | ±72 | 1784 | ±63 | 1876 | ±12 | 2702 | ±173 | +5 | 0.096 | 39 | 3.110 | 4.0 | 0.1148 | 0.7 | 5.09 | 4.1 | 0.3216 | 4.0 | 0.99 |

| | | | | | | | | | | | | | | | | | | | | | | | | | | | | | | | | |
|---|---|---|---|---|---|---|---|---|---|---|---|---|---|---|---|---|---|---|---|---|---|---|---|---|---|---|---|---|---|---|---|---|
| C.3.1 | -1.8E-4 | 19 | 0.1124 | 0.48 | 0.253 | 0.6 | 1.156 | 0.69 | – | 0.69 | 0.75 | 1798 | ±63 | 1786 | ±72 | 1748 | ±70 | 1878 | ±11 | 2315 | ±91 | +5 | 0.114 | 7 | 3.108 | 4.0 | 0.1149 | 0.6 | 5.10 | 4.1 | 0.3217 | 4.0 | 0.99 |
| C.23.1 | -2.7E-4 | 12 | 0.1115 | 0.78 | 0.017 | 1.6 | 1.101 | 1.65 | – | 0.05 | 0.63 | 1805 | ±61 | 1793 | ±70 | 1794 | ±62 | 1883 | ±15 | 3535 | ±201 | +5 | 0.081 | 104 | 3.095 | 3.9 | 0.1152 | 0.8 | 5.13 | 4.0 | 0.3231 | 3.9 | 0.98 |
| C.47.1 | -1.2E-3 | 12 | 0.1148 | 1.33 | 0.180 | 1.1 | 1.099 | 1.11 | – | 0.48 | 1.25 | 1810 | ±68 | 1760 | ±76 | 1742 | ±72 | 2105 | ±32 | 2836 | ±139 | +16 | 0.107 | 10 | 3.085 | 4.3 | 0.1305 | 1.8 | 5.83 | 4.7 | 0.3242 | 4.3 | 0.92 |
| C.12.1 | -1.8E-4 | 15 | 0.1113 | 0.97 | 0.015 | 1.8 | 1.132 | 0.55 | – | 0.04 | 0.64 | 1811 | ±63 | 1803 | ±72 | 1803 | ±63 | 1860 | ±18 | 3225 | ±193 | +3 | 0.093 | 110 | 3.084 | 4.0 | 0.1138 | 1.0 | 5.09 | 4.1 | 0.3243 | 4.0 | 0.97 |
| C.34.2 | -6.3E-4 | 15 | 0.1131 | 0.71 | 0.140 | 1.1 | 1.117 | 1.00 | – | 0.38 | 1.08 | 1812 | ±66 | 1785 | ±75 | 1769 | ±70 | 1978 | ±22 | 2630 | ±123 | +10 | 0.109 | 11 | 3.081 | 4.2 | 0.1215 | 1.2 | 5.44 | 4.4 | 0.3245 | 4.2 | 0.96 |
| C.36.1 | -1.1E-3 | 13 | 0.1144 | 0.87 | 0.134 | 1.2 | 0.988 | 1.09 | – | 0.37 | 1.18 | 1812 | ±68 | 1768 | ±76 | 1759 | ±70 | 2077 | ±28 | 2864 | ±147 | +15 | 0.101 | 12 | 3.081 | 4.3 | 0.1284 | 1.6 | 5.75 | 4.6 | 0.3246 | 4.3 | 0.94 |
| C.21.1 | -1.5E-3 | 10 | 0.1118 | 0.77 | 0.172 | 1.0 | 1.111 | 1.04 | – | 0.47 | 1.13 | 1826 | ±68 | 1776 | ±75 | 1753 | ±71 | 2117 | ±28 | 2938 | ±142 | +16 | 0.111 | 9 | 3.054 | 4.3 | 0.1314 | 1.6 | 5.93 | 4.6 | 0.3274 | 4.3 | 0.93 |
| C.6.1 | -2.1E-3 | 10 | 0.1066 | 0.89 | 0.175 | 2.5 | 1.028 | 1.20 | – | 0.49 | 1.27 | 1829 | ±63 | 1774 | ±70 | 1744 | ±66 | 2147 | ±35 | 3053 | ±163 | +17 | 0.115 | 9 | 3.048 | 4.0 | 0.1337 | 2.0 | 6.05 | 4.5 | 0.3281 | 4.0 | 0.89 |
| C.41.1 | -1.4E-3 | 10 | 0.1117 | 0.76 | 0.165 | 1.1 | 1.083 | 1.04 | – | 0.46 | 1.13 | 1830 | ±68 | 1783 | ±76 | 1762 | ±71 | 2104 | ±28 | 2890 | ±141 | +15 | 0.110 | 10 | 3.047 | 4.3 | 0.1304 | 1.6 | 5.90 | 4.6 | 0.3282 | 4.3 | 0.94 |
| C.5.1 | -1.6E-3 | 11 | 0.1119 | 0.84 | 0.153 | 1.2 | 1.043 | 1.15 | – | 0.41 | 1.25 | 1830 | ±69 | 1775 | ±77 | 1756 | ±72 | 2145 | ±32 | 3121 | ±163 | +17 | 0.110 | 11 | 3.047 | 4.4 | 0.1335 | 1.8 | 6.04 | 4.7 | 0.3282 | 4.4 | 0.92 |
| C.15.1 | -3.2E-4 | 19 | 0.1116 | 1.64 | 0.123 | 1.0 | 1.117 | 0.93 | – | 0.33 | 1.03 | 1832 | ±67 | 1822 | ±77 | 1800 | ±69 | 1893 | ±31 | 2529 | ±112 | +4 | 0.121 | 13 | 3.043 | 4.2 | 0.1158 | 1.7 | 5.25 | 4.5 | 0.3286 | 4.2 | 0.93 |
| C.22.1 | -1.3E-3 | 11 | 0.1109 | 0.79 | 0.407 | 2.1 | 1.066 | 1.09 | – | 1.06 | 1.21 | 1833 | ±68 | 1792 | ±77 | 1706 | ±81 | 2073 | ±29 | 2619 | ±124 | +13 | 0.122 | 6 | 3.041 | 4.3 | 0.1282 | 1.6 | 5.81 | 4.6 | 0.3288 | 4.3 | 0.93 |
| C.7.1 | -5.9E-4 | 13 | 0.1102 | 2.23 | 0.216 | 2.1 | 1.048 | 0.44 | – | 0.60 | 1.02 | 1838 | ±63 | 1823 | ±72 | 1785 | ±68 | 1929 | ±40 | 2466 | ±110 | +5 | 0.119 | 8 | 3.031 | 3.9 | 0.1182 | 2.2 | 5.38 | 4.5 | 0.3299 | 3.9 | 0.87 |
| C.26.1 | -1.1E-3 | 12 | 0.1085 | 0.76 | 0.149 | 1.1 | 1.114 | 1.03 | – | 0.41 | 1.13 | 1839 | ±68 | 1812 | ±77 | 1782 | ±71 | 2002 | ±27 | 2839 | ±138 | +9 | 0.122 | 10 | 3.029 | 4.3 | 0.1231 | 1.5 | 5.60 | 4.5 | 0.3301 | 4.3 | 0.94 |
| C.49.1 | -8.2E-4 | 11 | 0.1126 | 1.21 | 0.069 | 3.4 | 1.170 | 2.99 | – | 0.21 | 0.89 | 1839 | ±78 | 1811 | ±89 | 1808 | ±79 | 2008 | ±25 | 2939 | ±188 | +10 | 0.099 | 27 | 3.029 | 4.9 | 0.1235 | 1.4 | 5.62 | 5.1 | 0.3301 | 4.9 | 0.96 |
| C.43.1 | -8.1E-4 | 15 | 0.1331 | 1.60 | 0.126 | 1.3 | 1.339 | 1.21 | – | 0.35 | 1.33 | 2078 | ±78 | 2032 | ±93 | 2027 | ±81 | 2270 | ±31 | 3166 | ±164 | +10 | 0.111 | 21 | 2.629 | 4.4 | 0.1435 | 1.8 | 7.53 | 4.8 | 0.3803 | 4.4 | 0.92 |

Errors are 1-sigma; Pbc and Pb* indicate the common and radiogenic portions. respectively. Error in Standard calibration was 0.59% (not included in above errors but required when comparing data from different mounts). (1) Common Pb corrected using measured $^{204}$Pb. (2) Common Pb corrected by assuming $^{206}$Pb/$^{238}$U–$^{207}$Pb/$^{235}$U age-concordance. (3) Common Pb corrected by assuming $^{206}$Pb/$^{238}$U–$^{208}$Pb/$^{232}$Th age-concordance. Error in Standard calibration was 0.99% (not included in above errors but required when comparing data from different mounts)